APPENDIX

P1

Cytogenet Cell Genet 87:75–79 (1999)

Cytogenetics and Cell Genetics

Characterization and chromosome location of the mouse link protein gene *(Crtl1)*

F. Deák,[a] L. Mátés,[a] K. Krysan,[a] Z. Liu,[b] P.E. Szabó,[c] J.R. Mann,[c] D.R. Beier,[b] and I. Kiss[a]

[a] Institute of Biochemistry, Biological Research Center of the Hungarian Academy of Sciences, Szeged (Hungary);
[b] Brigham and Women's Hospital, Harvard Medical School, Boston, MA (USA); and
[c] Division of Biology, Beckman Research Institute of the City of Hope, Duarte, CA (USA)

Abstract. Link protein (LP) plays an essential role in endochondral bone formation by stabilizing the supramolecular assemblies of aggrecan and hyaluronan. We have isolated and characterized the mouse link protein gene (*Crtl1*). It is longer than 40 kb and transcribed from two alternative promoters, leading to heterogenous mRNAs between 5.3 and 1.3 kb in size. Apart from the coding sequence, the 5′ flanking region is also highly conserved in mammals. Immunostaining revealed high levels of LP expression in the cartilaginous primordia of skeletal elements and low levels in other tissues. Using single-strand conformation polymorphism analysis, *Crtl1* was assigned to mouse chromosome 13, tightly linked to *Dhfr*.

Cartilage performs its fundamental functions during embryonic development and in the adult via its highly organized extracellular matrix. The network of hyaluronan, aggrecan, and link protein (LP) macromolecular aggregates, embedded into a meshwork of type II collagen fibers, enables the tissue to withstand immense compressive load. Due to its mosaic structure, LP simultaneously interacts with aggrecan and hyaluronan, thus fulfilling a pivotal role in the formation of a very stable and compact ternary complex (reviewed by Neame and Barry, 1993). Inactivation of *Crtl1* leads to delayed endochondral bone formation and various skeletal abnormalities, causing dwarfism or postnatal lethality (Watanabe and Yamada, 1999). To get further insight into the function and regulation of LP, we isolated and sequenced the gene in the mouse, a key organism for gene targeting and transgenic animal models of human diseases. We also determined the map position of *Crtl1* on chromosome 13.

Materials and methods

Isolation and characterization of cDNA and genomic clones

A mouse epiphysis cDNA library (Deák et al., 1997) in λZAP-II vector was screened with a chicken LP cDNA probe (Deák et al., 1986) to isolate the clone pLPm17. Clone IMAGp998N211035, for the mouse expressed sequence tag (EST) AA008559, was obtained from the Resource Center (Berlin-Charlottenburg, Germany). Genomic clones were isolated from a mouse 129/Sv genomic library in λFixII vector (Stratagene) using mouse LP cDNA fragments. In addition, clone pD283 was made by the polymerase chain reaction (PCR) using rat LP primers Pr1 (5′-CCA ATC AAA GGT GGC TCT GT-3′) and Pr2 (5′-TTT GAT TTT ATG ACA TCA CAC TGG-3′), sequenced directly, and cloned. DNA sequences were determined on both strands using a Dye Terminator Cycle Sequencing Kit (Perkin-Elmer) and an ABI373 automatic DNA sequencer.

RNA from guanidinium thiocyanate extracts of epiphyseal cartilage of newborn mice was sedimented through a cesium trifluoroacetate cushion and enriched in poly(A)$^+$ RNA using oligo(dT) magnetic beads (Dynal). The transcription start points were determined essentially as described previously (Deák et al., 1991): (1) primers Pr3 (5′-TTG TCC TGA ATT CCA GTT CAG A-3′) and Pr4 (5′-GCA CTC CAT GCA AAC TTC AG-3′) were elongated with M-MLV reverse transcriptase (GIBCO BRL); (2) the gene-specific reverse primer Pr5 (5′-GGT GAC GCT TTG CTT TCT TC-3′) was extended with T4 DNA polymerase on a single-stranded genomic DNA template annealed to the mRNA, and the products were separated on a sequencing gel.

Supported by the US-Hungarian Science and Technology Joint Fund under Project J.F. No. 633, Grant OTKA M027770 providing equipment to I.K. and Grant No. DK45639 to D.B.

Received 11 May 1999; revision accepted 24 August 1999.

Request reprints from Dr. Ibolya Kiss, Institute of Biochemistry, Biological Research Center of the Hungarian Academy of Sciences, PO Box 521, H-6701 Szeged (Hungary); telephone: 36-62-432-232; fax: 36-62-433-506 or 36-62-432 576; e-mail: Kiss@nucleus.szbk.u-szeged.hu

KARGER

Fax + 41 61 306 12 34
E-mail karger@karger.ch
www.karger.com

0301–0171/99/0872–0075$17.50/0

Accessible online at:
www.karger.com/journals/ccg

Immunohistochemistry on unfixed cryogenically frozen sections of mouse embryos was performed as described elsewhere (Deák et al., 1997), using an antiserum made against bovine link protein (Franzén et al., 1981). Preimmune serum was used as a negative control.

Chromosome localization

To test for single-strand conformation polymorphisms (SSCPs) between mouse strains, as previously described (Brady et al., 1997), primers were designed to amplify an intronic region of *Crtl1*. Oligonucleotides were radiolabeled with [^{32}P]ATP using polynucleotide kinase, and genomic DNAs from a series of mouse strains were amplified using standard protocols. Two microliters of the amplified reaction was added to 8.5 µl USB stop solution, denatured at 94 °C for 5 min, and immediately placed onto ice. Two microliters of each reaction was loaded on a 6% nondenaturing acrylamide sequencing gel and electrophoresed in 0.5 × TBE buffer for 2–3 h at 40 W in a 4 °C cold room. A primer pair, Pr6 (5′-GCC AAA ACA CGG TGC CT-3′) and Pr7 (5′-GCT TGC ACC GCC TCA TCG TAG-3′), identified a polymorphism between C57BL/6J and *Mus spretus* and was used to analyze DNA prepared from the BSS backcross (Rowe et al., 1994). The strain distribution pattern was analyzed using Map Manager (Manly et al., 1993).

Results and discussion

We have isolated cDNA and genomic clones for mouse LP using a combination of various strategies. The clone pLPm17, isolated from an epiphysis cDNA library using a chicken cDNA probe, encodes the second hyaluronan-binding module and 250-bp 3′-untranslated sequence of *Crtl1*. It recognizes mouse mRNA species of 5.3, 4.6, 2.7, 2.1, 1.5, and 1.3 kb in Northern blot analysis. Heterogenous mRNAs within a similar size range were described for rat and human LPs (Neame and Barry, 1993; Dudhia et al., 1994), and somewhat larger mRNAs encode the chicken protein (Deák et al., 1986). EST AA008559, which is related to pLPm17, was found in a BLAST sequence similarity search, and analysis of the corresponding clone revealed that the mouse LP precursor consists of 356 amino acids (GenBank accession number AF139572). Its primary sequence is extremely conserved, showing 99%, 97%, and 91% identity with LP sequences from rat, human, and chicken, respectively (Fig. 1). In fact, the mouse protein differs from the rat counterpart only by two conservative replacements in the signal peptide, the insertion of two residues into the NH_2 terminus of the mature protein, and a single conservative replacement in the immunoglobulin (Ig)-like module. In general, the sequence diversity among vertebrate species is highest in the first 16 residues of the mature LP. Conversely, the degree of sequence conservation is highest in the repeated hyaluronan-binding modules (HAB1 and HAB2), where, out of 197 moieties, only the chicken sequence shows, altogether, six conservative changes. Apart from the Cys residues, amino acids, which comprise the consensus hydrophobic core of the predicted hyaluronan-binding site of TSG-6 and other hyaluronan-binding proteins (Kohda et al., 1996), are also fully conserved in LP sequences from different species (Fig. 1).

Three independent clones encoding exon 2 and, altogether, five clones covering exons 3–5 were isolated from a mouse 129/Sv genomic library. The two sets of clones do not overlap (Fig. 2). The 5′ end of the gene was amplified and cloned using the rat-derived primers Pr1 and Pr2. Based on restriction mapping and genomic Southern blot analysis, introns A and B are

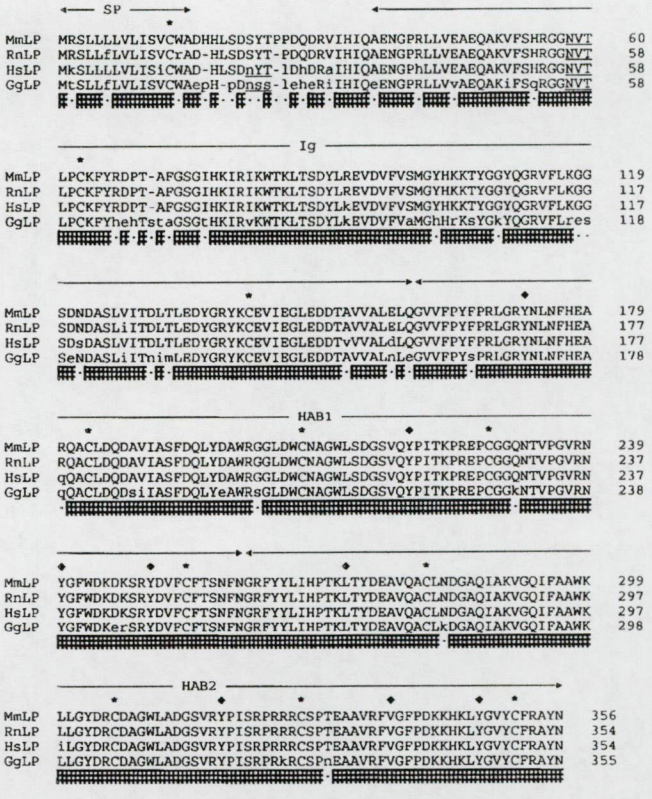

Fig. 1. Alignment of the amino acid sequence of mouse link protein to those from other species. Mouse (MmLP), rat (RnLP) (Neame et al., 1986), human (HsLP) (Dudhia and Hardingham, 1990), and chicken (GgLP) (Deák et al., 1986) sequences are compared. Horizontal arrows indicate the extension of modules. Asterisks mark the conserved Cys residues. Diamonds depict the conserved motifs comprising the consensus hydrophobic core of the predicted hyaluronan-binding site of TSG-6 and other related proteins (Kohda et al., 1996). SP = signal peptide, Ig = immunoglobulin-like module, HAB1 and HAB2 = hyaluronan-binding modules.

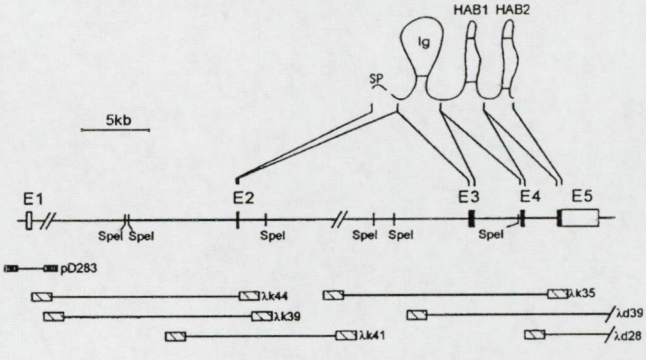

Fig. 2. Exon-intron structure of *Crtl1*. Translated and untranslated exons (E1–E5) are marked by closed and open boxes, respectively. Location of the genomic clones is depicted below and the schematic domain structure of the protein is shown above the gene. Symbols as in Fig. 1; kb = kilobase pairs.

larger than 15 and 16 kb, respectively, and thus the gene is longer than 40 kb. Nucleotide sequences of the exons and the neighboring regions (GenBank accession numbers AF137274 through AF137278) revealed phase I introns bordered with conforming splice sites, conserved exon sizes (Table 1), and an

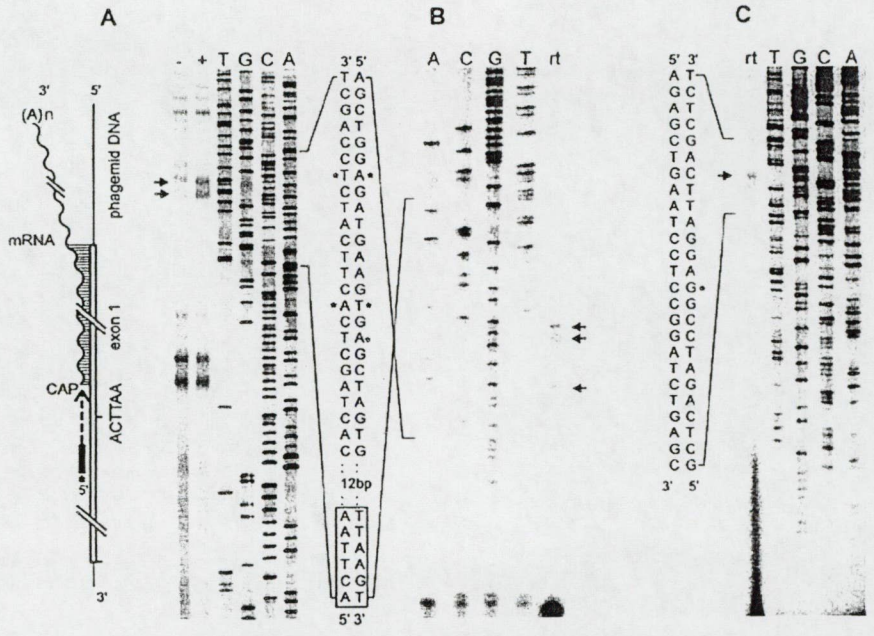

Fig. 3. Mapping of the transcription start sites of *Crtl1;* 2.5 μg of poly(A)⁺ RNA was used. The 5′-end labeled oligonucleotides were elongated and run along the sequencing ladders from the same primers, and the start points identified are marked (*) in the sequence. (**A**) Extension of primer Pr5 by T4 DNA polymerase on the single-stranded genomic DNA-mRNA hybrid template. The diagram to the left depicts the experimental strategy. In lane (+), LP mRNA specifically blocks primer extension at two positions indicated by arrowheads. In the control lane (–), tRNA was added instead of poly(A)⁺ RNA. (**B**) Extension of primer Pr3 by reverse transcriptase (lane rt). Note that the opposite strand is shown as in **A**. (**C**) Extension of primer Pr4 by reverse transcriptase.

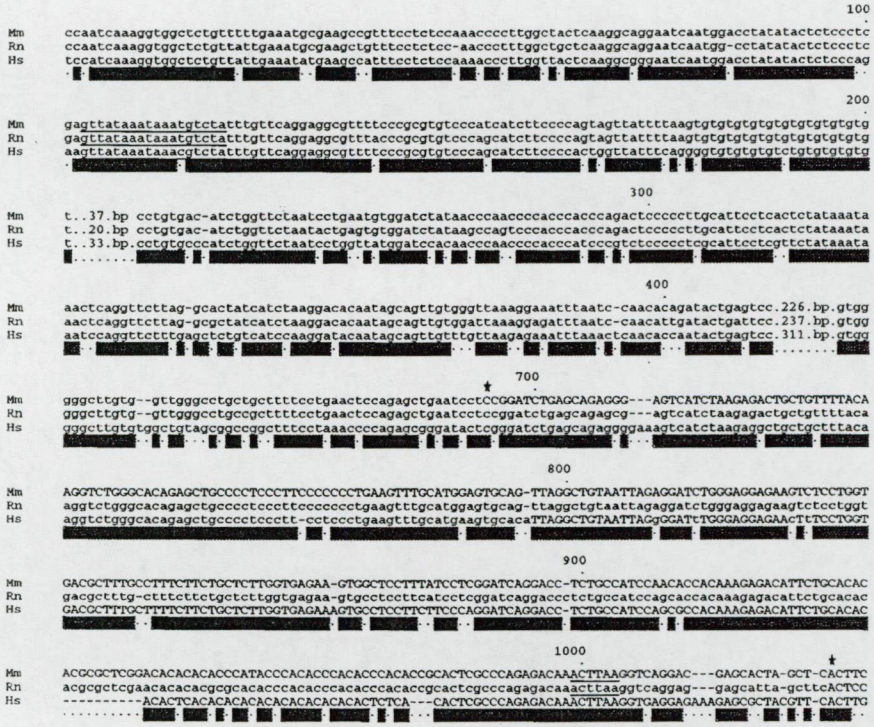

Fig. 4. Nucleotide sequence of the 5′ end of the gene. Mouse, rat (Rhodes et al., 1991), and human (Dudhia et al., 1994) sequences are aligned. Exons are indicated by uppercase letters. Mouse LP start sites are denoted by asterisks, while the conserved AT-rich sequence and the TATA-like ACTTAA motifs are underlined.

exon-intron structure (Fig. 2) similar to that of the chicken (Kiss et al., 1987) or human gene (Dudhia et al., 1994).

Transcription start sites of *Crtl1* were mapped by reverse transcription and primer extension with T4 DNA polymerase (Fig. 3). A TATA-like motif, ACTTAA, precedes the two start points identified within the CACTTC and CATCTC motifs, both similar to CANYYY, the consensus sequence for eukaryotic start sites (Figs. 3A, B and 4). The same motif with a single start site was defined as the promoter for rat chondrosarcoma LP (Rhodes et al., 1991) (Fig. 4). However, only the

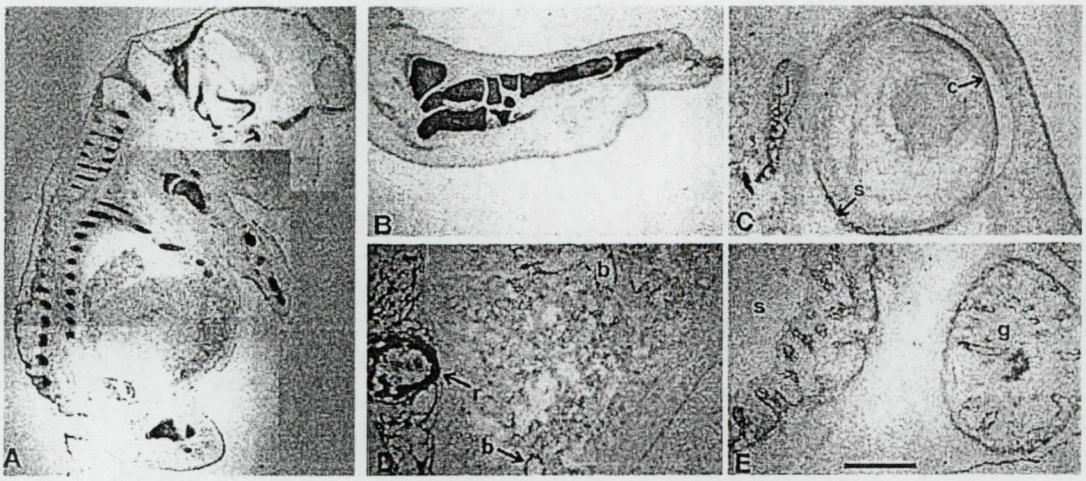

Fig. 5. Immunolocalization of LP during mouse development. Parasagittal sections of day 14.5 (**A**) and day 16.5 (**B–E**) post-conception embryos are shown. In sections of the whole embryo (**A**) and hind limb (**B**), all cartilage primordia of the skeletal bones are strongly stained. In the eye (**C**), staining of the conjunctiva (c) and sclera (s) can be observed, although less intensely than the cartilage primordium of the zygomatic bone (j). In the thorax (**D**), the most intense signal is produced by the cartilage primordium of rib and the periosteal collar of bone (r). Lung bronchioli (b) also showed a positive reaction. In the abdomen (**E**), staining of glandular epithelium lining the stomach (s) and midgut (g) can be observed. Bar: 1 mm in **A** and **B**, 400 μm in **C**, and 250 μm in **D** and **E**.

Table 1. Comparison of exon-intron structures of mouse and chicken link protein genes

Species	Exon	Size (bp)	5′ splice site	Intron	Size (kb)	3′ splice site
Mouse	1	392	ACAAGgtaaaact	A	>15	atccttacagCAGAG
Chicken[a]		504	ACAAGgtaaagaa		>33	gcccttacagTGAAG
Mouse	2	130	TCAAGgtaaggga	B	>16	ctcattatagCAGAA
Chicken		126	CCAAGgtaaggaa		>39	tgaattgtagAAGAA
Mouse	3	372	ACAAGgtaggtat	C	3.4	ctttgaatagGTGTG
Chicken		375	GGAAGgtaggtaa		11.6	gccatttcagGTGTT
Mouse	4	303	CAACGgtaagaca	D	2.4	ctccccatagGCCGA
Chicken		303	CAATGgtaagaac		7.2	ctctccccagGTCGT
Mouse	5	>3,000				
Chicken		4,800				

[a] Source: Kiss et al. (1987).

TATA-like motif is conserved in the human sequence, and the transcription from CRTL1 initiates 191 bp upstream. Reverse transcription-coupled PCR indicated the presence of a mouse LP mRNA fraction protruding further into 5′ direction (not shown). The corresponding start site was mapped by the extension of primer Pr4 (Figs. 3C and 4), thus defining 392 bp for the length of exon 1 (Table 1) and a weak, TATA-less upstream promoter. Interestingly, the sequence conservation in the 5′-flanking region is also high between mammalian species (Fig. 4) and includes an AT-rich element, which was previously shown to mediate glucocorticoid responsiveness in the 5′ control region of the rat gene (Rhodes and Yamada, 1995).

Accumulation of LP was monitored in mouse embryos using antiserum against bovine LP (Fig. 5). All the cartilaginous elements of the developing skeleton exhibited intense staining. Immunostaining in noncartilaginous tissues was also observed, including the sclera and conjunctiva of the eye, bronchiolar lung tissue, the mucosa of the stomach and midgut, and metanephric tissue. These findings agree with earlier observations in chicken noncartilaginous tissues (Neame and Barry, 1993), suggesting a general role for LP in the stabilization of the interaction between large aggregating proteoglycans and hyaluronan in other tissues as well.

The phenotypic consequences of inactivation of *Crtl1* have been shown recently in transgenic mice (Watanabe and Yamada, 1999), but developmental disorders associated with human or mouse LP have not yet been described. To facilitate the identification of naturally occurring mutations in mice, we mapped the chromosomal location of *Crtl1* using SSCP analysis. An SSCP was identified between inbred mouse strains within intron D. The BSS interspecific backcross was genotyped and the allele distribution pattern analyzed using Map Manager (Fig. 6). We mapped *Crtl1* to chromosome 13 with a lod likelihood score of 28. No recombinants between *Crtl1* and

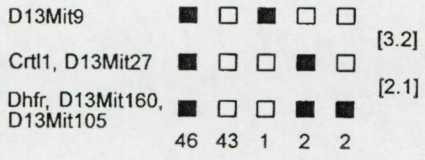

Fig. 6. Chromosome location of the mouse *Crtl1* gene. Haplotypes of the region surrounding *Crtl1* on chromosome 13 in 94 progeny of the BSS cross are shown. Filled boxes represent the C57BL/6J allele; open boxes represent *Mus spretus*. Nine *Dhfr* genotypes were inferred from flanking markers. Numbers in brackets indicate distances in centimorgans.

the marker *D13Mit27* were found among 94 progeny. The position of *Crtl1* with respect to flanking microsatellite markers is: *D13Mit9* – 3.19 ± 1.81 cM – *D13Mit27, Crtl1* – 2.13 ± 1.49 cM – *Dhfr, D13Mit160, D13Mit105*. Therefore, we concluded that *Crtl1* is tightly linked to *Dhfr* on mouse chromosome 13. These results are consistent with the localization of STSs (sequence tagged sites) derived from the human homologs of *Crtl1* (sts-G42790, sts-W92748) and *Dhfr* (sts-AA010576) to the long arm of chromosome 5 on the human transcript map (http://www.ncbi.nlm.nih.gov/genemap98; Deloukas et al., 1998). Interestingly, however, CRTL1 maps to the interval between D5S656 (121.6 cM) and D5S471 (129.6 cM), corresponding to 5q21, whereas DHFR maps to the interval between D5S1977 (82.2 cM) and D5S428 (95.4 cM), corresponding to 5q13. Additionally, the gene *Cspg2*, which encodes versican and is distantly related to LP, maps to a neighboring site on the same chromosome and is located 1 cM proximal to *Dhfr* (Naso et al., 1995; Meersseman et al., 1997). Human CSPG2 also maps to the interval between D5S1977 and D5S428.

Acknowledgements

We thank D. Heinegard for the gift of antiserum against bovine LP. We also thank I. Fekete and A. Simon for excellent technical assistance.

References

Brady KP, Rowe LB, Her H, Stevens TJ, Eppig J, Sussman DJ, Sikela J, Beier DR: Genetic mapping of 262 loci derived from expressed sequences in a murine interspecific cross using single-strand conformational polymorphism (SSCP) analysis. Genome Res 7:1085–1093 (1997).

Deák F, Barta E, Mestric S, Biesold M, Kiss I: Complex pattern of alternative splicing generates unusual diversity in the leader sequence of the chicken link protein mRNA. Nucl Acids Res 19:4983–4990 (1991).

Deák F, Kiss I, Sparks KJ, Argraves WS, Hampikian G, Goetinck PF: Complete amino acid sequence of chicken cartilage link protein deduced from cDNA clones. Proc natl Acad Sci, USA 83:3766–3770 (1986).

Deák F, Piecha D, Bachrati C, Paulsson M, Kiss I: Primary structure and expression of matrilin-2, the closest member of cartilage matrix protein within the von Willebrand factor type A-like module superfamily. J biol Chem 272:9268–9274 (1997).

Deloukas P, Schuler GD, Gyapay G, Beasley EM, Soderlund C, Rodriguez-Tome P, Hui L, Matise TC, McKusick KB, Beckmann JS, Bentolila S, Bihoreau M, Birren BB, Browne J, Butler A, Castle AB, Chiannilkulchai N, Clee C, Day PJ, Dehejia A, Dibling T, Drouot N, Duprat S, Fizames C, Fox S, Gelling S, Green L, Harrison P, Hocking R, Holloway E, Hunt S, Keil S, Lijnzaad P, Louis-Dit-Sully C, Ma J, Mendis A, Miller J, Morissette J, Muselet D, Nusbaum HC, Peck A, Rozen S, Simon D, Slonim DK, Staples R,. Stein LD, Stewart EA, Suchard MA, Thangarajah T, Vega-Czarny N, Webber C, Wu X, Hudson J, Auffray C, Nomura N, Sikela JM, Polymeropoulos MH, James MR, Lander ES, Hudson TJ, Myers RM, Cox DR, Weissenbach J, Boguski MS, Bentley DR: A physical map of 30,000 human genes. Science 282:744–746 (1998).

Dudhia J, Bayliss MT, Hardingham TE: Human link protein gene: structure and transcription pattern in chondrocytes. Biochem J 303:329–333 (1994).

Franzén A, Björnsson S, Heinegård D: Cartilage proteoglycan aggregate formation: role of link protein. Biochem J 197:669–674 (1981).

Kiss I, Deák F, Mestric S, Delius H, Soós J, Dékány K, Argraves WS, Sparks KJ, Goetinck PF: Structure of the chicken link protein gene: exons correlate with the protein domains. Proc natl Acad Sci, USA 84:6399–6403 (1987).

Kohda D, Morton CJ, Parkar AA, Hatanaka H, Inagaki FM, Campbell ID, Day AJ: Solution structure of the link module: a hyaluronan-binding domain involved in extracellular matrix stability and cell migration. Cell 86:767–775 (1996).

Manly KF: A Macintosh program for storage and analysis of experimental genetic mapping data. Mammal Genome 4:303–313 (1993).

Meersseman G, Verschueren K, Nelles L, Blumenstock C, Kraft H, Wuytens G, Remacle J, Kozak CA, Tylzanowski P, Niehrs C, Huylebroeck D: The C-terminal domain of Mad-like signal transducers is sufficient for biological activity in the *Xenopus* embryo and transcriptional activation. Mech Dev 61:127–40 (1997).

Naso MF, Morgan JL, Buchberg AM, Siracusa LD, Iozzo RV: Expression pattern and mapping of the murine versican gene (*Cspg2*) to chromosome 13. Genomics 29:297–300 (1995).

Neame PJ, Barry FP: The link proteins. Experientia 49:393–402 (1993).

Rhodes C, Savagner P, Line S, Sasaki M, Chirigos M, Doege K, Yamada Y: Characterization of the promoter for the rat and human link protein gene. Nucl Acids Res 19:1933–1939 (1991).

Rhodes C, Yamada Y: Characterization of a glucocorticoid responsive element and identification of an AT-rich element that regulates the link protein gene. Nucl Acids Res 23:2305–2313 (1995).

Rowe LB, Nadeau JH, Turner R, Frankel WN, Letts VA, Eppig JT, Ko MSH, Thurston SJ, Birkenmeier EH: Maps from two interspecific backcross DNA panels available as a community genetic mapping resource. Mammal Genome 5:253–274 (1994).

Watanabe H, Yamada Y: Mice lacking link protein develop dwarfism and craniofacial abnormalities. Nature Genet 21:225–229 (1999).

P2

ELSEVIER

Matrix Biology 21 (2002) 163–174

MATRIX BIOLOGY

www.elsevier.com/locate/matbio

Comparative analysis of the mouse and human genes (*Matn2* and *MATN2*) for matrilin-2, a filament-forming protein widely distributed in extracellular matrices☆

Lajos Mátés[a], Éva Korpos[a], Ferenc Deák[a], Zhanqin Liu[b], David R. Beier[b], Attila Aszódi[c], Ibolya Kiss[a,*]

[a]*Institute of Biochemistry, Biological Research Center of the Hungarian Academy of Sciences, P.O. Box 521, H-6701 Szeged, Hungary*
[b]*Brigham and Women's Hospital, Harvard Medical School, Boston, MA, USA*
[c]*Department of Experimental Pathology, Lund University, S-22185 Lund, Sweden*

Received 17 August 2001; accepted 9 November 2001

Abstract

We previously identified matrilin-2 (MATN2), the largest member of the novel family of matrilins. These filament-forming adapter proteins expressed in a distinct, but partially overlapping, pattern in all tissues were implicated in the organization of the extracellular matrix. Matrilin-2 functions in a great variety of tissues. Here, we present the genomic organization of the highly conserved mouse and human *MATN2* loci, which cover >100 kb and 167.167 kb genomic regions, respectively, and are composed of 19 exons. RT-PCR analysis revealed that alternative transcripts with identical protein coding regions are transcribed from two promoters in both species. The upstream, housekeeping type promoter is functional in all tissues and cell types tested. The activity of the downstream, TATA-like promoter preceded with putative motifs for the homeobox transcription factor PRRX2 is restricted to embryonic fibroblasts and certain cell lines. The oligomerization module is split by an U12-type AT-AC intron found in conserved position in all four matrilin genes. We assigned *Matn2* to mouse chromosome 15, linked to *Trhr* and *Sntb1* in a region synthenic to human chromosome 8q22-24.

Keywords: Extracellular matrix; Adapter protein; Genomic organization; AT-AC introns; Alternative promoters; PRRX2 motifs

1. Introduction

Matrilin-2 is a member of the novel family of multiadhesion proteins, the matrilins (Deák et al., 1997, 1999b). The members of this family are composed of one or two von Willebrand factor A (vWFA) domains, varying number of epidermal growth factor-like (EGF) modules and a C-terminal coiled coil oligomerization domain (Deák et al., 1999b). They function in the extracellular matrix (ECM) assembly of various tissues forming both collagen-associated and collagen-independent filamentous networks (Chen et al., 1999; Piecha et al., 1999; Klatt et al., 2000, 2001). While matrilin-1 and -3 are abundant ECM components in skeletal elements, matrilin-2 and -4 function in a great variety of tissues (Deák et al., 1999b; Piecha et al., 1999; Klatt et al., 2000, 2001).

Although the precise role of matrilins in the ECM assembly has not been defined yet, recent data demonstrate the important role of matrilin-1 and -3 in the cartilaginous matrix. Matrilin-1, the best-characterized member of the family, was reported to interact with $\alpha_1\beta_1$ integrin (Makihira et al., 1999) and ECM ligands.

Abbreviations: bp, base pair; ECM, extracellular matrix; EGF, epidermal growth factor-like; EST, expressed sequence tag; kb, kilobase pairs; MED, multiple epiphyseal dysplasia; nt, nucleotide; PAC, P1 derived artificial chromosome; RACE, rapid amplification of cDNA ends; RT, reverse transcription; SSCP, single strand conformation polymorphism; UTR, untranslated region; vWFA, von Willebrand factor A.

☆ Nucleotide sequences reported in this paper have been deposited with the DDBJ/EMBL/GenBank Data Libraries under the Accession Numbers AF358830-AF358844.

* Corresponding author. Tel.: +36-62-432-232; fax: +36-62-433-506.

E-mail address: kiss@nucleus.szbk.u-szeged.hu (I. Kiss).

0945-053X/02/$ - see front matter
PII: S0945-053X(01)00194-9

As a fraction of matrilin-1 is covalently bound to aggrecan (Hauser et al., 1996), and matrilin-1 also decorates the type II collagen fibrils (Winterbottom et al., 1992), it was proposed to play a bridging role between the two main ECM networks of cartilage. Furthermore, deletion analysis demonstrated that matrilin-1 can form collagen-independent pericellular filaments via the vWFA domains (Chen et al., 1999). Mutations in the metal ion-dependent adhesion site of matrilin-1 interfered with the network formation, suggesting the involvement of an adhesion mechanism similar to that proposed for integrin–ligand interactions (Lee et al., 1995; Chen et al., 1999). Although ablation of the matrilin-1 gene altered only the collagen fibrillogenesis and failed to produce any obvious skeletal abnormalities (Aszódi et al., 1999; Huang et al., 1999), dominant negative mutation in the vWFA domain of matrilin-3 led to multiple epiphyseal dysplasia (MED) in human (Chapman et al., 2001).

Cloning and analysis of the cDNA for mouse and human matrilin-2 revealed the most complex domain structure among matrilins (Deák et al., 1997; Muratoglu et al., 2000). The monomer (104 kDa) contained two vWFA domains separated by 10 EGF modules, a unique segment not found in other proteins and a C-terminal α-helical coiled coil domain. In tissue extracts and cell line cultures, matrilin-2 was demonstrated to exist as a mixture of mono-, di-, tri- and tetramers using SDS-polyacrylamide gel electrophoresis and electron microscopy (Piecha et al., 1999). Based on the similarity of its domain structure to matrilin-1, matrilin-2 may also interact with collagens and proteoglycans and perform an adapter function in the ECM assembly of a variety of tissues. Expression of the mouse gene was detected by immunostaining in loose and dense connective tissues, subepithelial connective tissue of the skin and digestive tract and in certain skeletal structures. In situ hybridization revealed matrilin-2 mRNA expression in fibroblasts, smooth muscle cells and certain epithelial cells (Piecha et al., 1999).

To get insight into the regulation of gene expression and to provide a tool for functional studies using gene targeting, we isolated and characterized genomic clones for matrilin-2. Here we report the cloning, characterization and chromosome location of the mouse matrilin-2 gene (*Matn2*), and the genomic organization and comparative analysis of the human gene (*MATN2*) within the corresponding human contig. In addition, we have identified the transcription start points and putative *cis* regulatory elements and provided evidence that both genes are transcribed from alternative promoters. The upstream, housekeeping-like promoter is active in all cell types tested, while the downstream, TATA-like promoter functions only in embryonic fibroblasts and in certain cell lines.

2. Results

2.1. Molecular cloning and sequence analysis of the mouse matrilin-2 gene

Screening of a mouse 129/Sv genomic library with matrilin-2 cDNA probes covering the protein coding region and 250-bp 5′-untranslated region (UTR) (Deák et al., 1997) yielded altogether seven different λ clones designated λgMTR1-λgMTR5, λgMTR8 and λgMTR11 (Fig. 1b). Restriction mapping, subcloning and Southern hybridization with various cDNA fragments and gene-specific oligonucleotides revealed the locations of exons within the clones (Fig. 1b). Finally, the exons were identified by sequencing and alignment of genomic and cDNA sequences. Even though the λ clones overlapped with each other only at the 16-kb 3′ end of the locus, they carried the entire coding region with the exception of exon 4 and the untranslated exon 1 (Fig. 1a,b). We performed inverse PCR with exon 1-specific primers (Table 1) to amplify and clone the 5′ end of *Matn2* (pEx1 in Fig. 1b). Thereafter, six additional overlapping clones were found during the screening of a PAC library with pEx1 probe. Southern hybridization with various exon-specific probes and partial sequencing confirmed that PAC477-O13 covers not only the 5′ end, but the entire gene as well (Fig. 1b).

The complete *Matn2* contains 19 exons and spans more than 100 kb of genomic DNA (Fig. 1b). Exon 2 carries the translation start codon. The entire exon 1 and the major part of exon 19 consist of UTR. Exon 3 codes for the entire first vWFA domain, but the second vWFA domain is encoded by two exons (exons 14–15). Each of the EGF modules are encoded by separate exons, but also two exons code for each of the unique segment and the coiled coil oligomerization domain (Table 2). The exons range in length from 72 to 570 bp, while the introns range from 240 bp to more than 17 kb (Table 2). While the 3′ end is relatively compact, the introns are generally larger at the 5′ end. The length of introns B, C, D, F and J exceeded the value that we could determine by PCR. All the introns have phase I, and except for the last intron, they are bordered by consensus U2-type GT-AG splice sites (Sharp and Burge, 1997). Interestingly, however, the last intron is bordered by motifs characteristic for the rare class of AT-AC introns (Tables 2 and 3), which are excised by the minor spliceosome utilizing U11 and U12 snRNA (Tarn and Steitz, 1996). Previously, we showed mRNA heterogeneity at the C-terminal end of the coding region of *Matn2* (Piecha et al., 1999). Comparison of the cDNA and the genomic sequence revealed that usage of an alternative 3′ splice site resulted in the synthesis of a

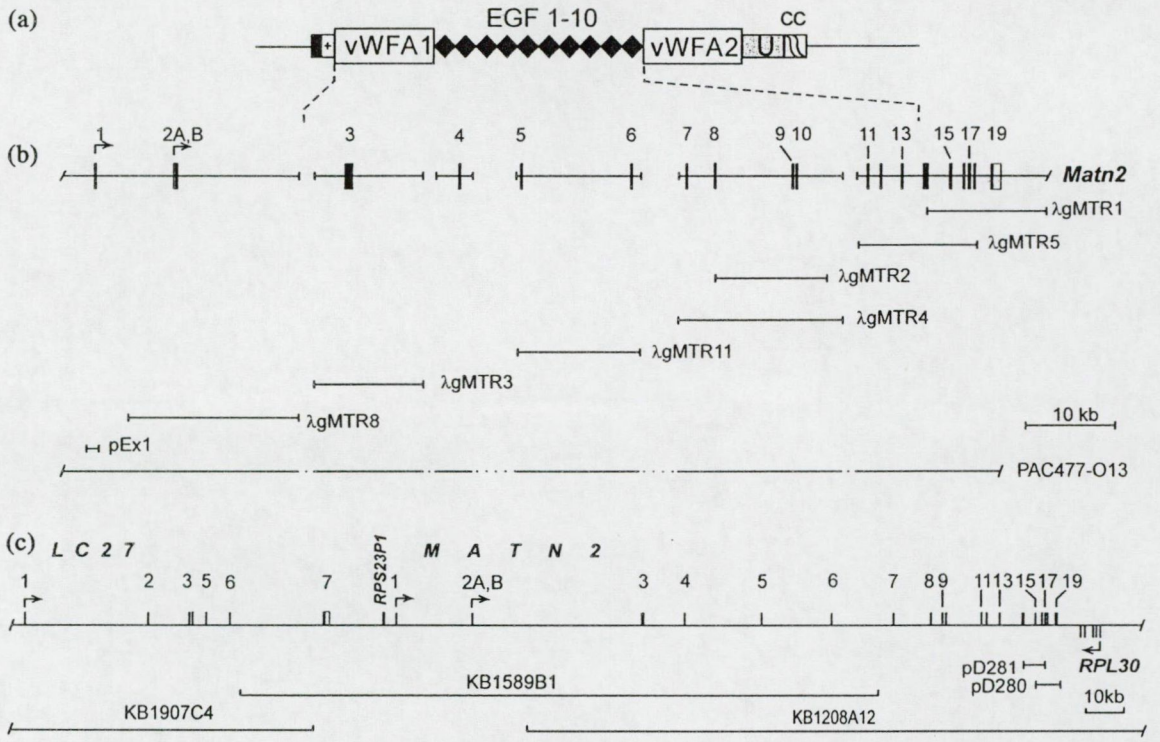

Fig. 1. Organization of the mouse and human genes for matrilin-2. (a) Modular structure of the protein. (b) Exon–intron structure of *Matn2*. Location of genomic λ clones, recombinant plasmid and PAC clones is depicted below the map. (c) Schematic representation of the *MATN2* locus. Genomic regions carried by recombinant plasmids and BAC clones are shown below. *LC27* and *RPL30* code for a putative, integral membrane transporter and ribosomal protein L30, respectively. *RPS23P1* is a pseudogene for S23 ribosomal protein.

protein isoform, which lacked 19 amino acids from the unique segment.

2.2. *Organization of the human gene (MATN2)*

Previously, we cloned the full-length *MATN2* cDNA from the permanent cell line HEp-2 (Muratoglu et al., 2000). Sequence alignment with the mouse homologue revealed large similarity between the two cDNAs, but different 5′-UTR. Using the human cDNA sequence, we searched for similarity in established databases. Two genomic clones, completely sequenced, and several ESTs were found. The two BAC clones, KB1589B1 and KB1208A12 (Accession Nos. AP002906 and AP003352) overlapping by 86900 bp, covered the whole *MATN2* (Fig. 1c). Sequence comparison with the EST sequence (Accession No. BF347123) protruding farthest into 5′ direction led us to determine the position of exon 1. GENSCAN analysis of the contig revealed 3 kb upstream of *MATN2* a single, 500-bp segment, that may encode a protein, which is 88% similar to the human S23 ribosomal protein (Accession No. XM_004020). Several hundred EST entries were found identical with the authentic *RPS23*, but all differed from the putative gene sequence in the same positions. Therefore, we concluded that the homologous region is a novel pseudogene for the S23 ribosomal protein, *RPS23P1* (Fig. 1c). This conclusion was further confirmed by the finding that *RPS23* on human chromosome 5 contains four exons, while *RPS23P1* is intronless and it contains part of the poly(A) tail, suggesting that the pseudogene presumably derived from an mRNA intermedier. 12 kb further upstream, GENSCAN analysis revealed the last exon of *LC27* encoding a putative transmembrane protein (Accession No. XM 011642). The rest of *LC27* carried by BAC clone KB1907C4 (Accession No. AP003357) spans a 77-kb interval. *LC27* and *RPS23P1* are tandemly arranged with *MATN2* (Fig. 1c). At the 3′ vicinity of *MATN2*, *RPL30* encoding the L30 ribosomal protein is situated in the opposite orientation.

The complete *MATN2* is 167167 bp long and has the same exon–intron structure as the mouse orthologue (Fig. 1). Phase I introns are located in conserved positions in both genes, and the exon–intron junction sequences are also highly conserved, including all the GT-AG and the last, AT-AC splice sites (Table 2). Our data confirm that AT-AC introns with highly similar splice junction sequences are located in conserved positions in all matrilin genes sequenced to date from any species (Table 3). Thus, the matrilin genes belong to the rare class of eukaryotic genes spliced by the U12-type minor spliceosome. The lengths of protein coding

Table 1
Oligonucleotide primer sequences

Name	Sequence	Position
Mouse primers[a]		
pAr	CGGACGCGAACAAGAATC	119–102[b]
pBr	GCTCCTTGGGCACCGATCC	139–121[b]
pCr	GCCCCGCAGAGGACCGCAGA	159–140[b]
pDn	GCGGACCACGGAGACTGA	166–183[b]
pEn	GCTGCTCCCCTGTCTCTC	192–209[b]
pFn	CCCTGCCAGCTCAAGAGAAC	4667–4686[c]
pGn	CTGAAAAATCAGGGCAATGG	4762–4781[c]
pHn	AACATCAGGGACACCCAGAAA	4796–4816[c]
pIn	CAGCCCTGCTCCTCTTGAA	241–259[b]
pJr	CAGTGCAGTCTGCGGATACA	398–379[b]
pKr	TCTGCCCGCTTATTCTCACA	430–411[b]
pLr	GGAGCAGACCTACTCGGGTAA	558–538[b]
pMr	CTTGACCGTGCTGCCATATT	578–559[b]
pNn	CATTGACAAGCATCTCTTCT	2687–2706[b]
pOr	TTTGTGTAGACCGTGAAAGA	2949–2930[b]
pPr	CGTTCTGGAACAGTATAAGG	3039–3020[b]
Human primers		
pQn	AGGCCGACGAGGAAGACC	41941–41958[d]
pRn	CCAACTATGCATGCCCTGCT	60583–60603[d]
pSn	AAGCTCTCAAAGGCCAAACA	60641–60650[d]
pTn	TGAGTGCAAGTGGTCTGTTTG	60675–60695[d]
pVn	GGTCACGTGGGAGGTCCA	202–219[e]

[a] pKr and pMr were also used for RT-PCR on human template.
[b] Positions are given from start of the longest transcript or as under Accession Numbers:
[c] AF358831;
[d] AP002906;
[e] U69263.

exons of *MATN2* are identical with those of *Matn2* (Table 2), only the UTRs of exons 1 and 19 show some length variability. Interestingly, however, the sequence of human and mouse cDNA clones (Deák et al., 1997; Muratoglu et al., 2000) differed in the 5′-UTR. Aligning the sequences of the genomic clones with those of the mouse RACE clones pCRP233 and pCRP207 (Deák et al., 1997), as well as with EST entries from both species, defined a common region (designated exon 2B in Table 2) with a length of 165 and 168 bp in the mouse and human, respectively. The human RACE clone pMTNh-5 reported recently (Muratoglu et al., 2000), however, overlapped with the genomic sequence upstream of exon 2B in a region designated as exon 2A (Table 2). Furthermore, the segment of *Matn2* preceding exon 2B also exhibited high degree of sequence similarity to exon 2A of *MATN2* (see later, Fig. 4b). This suggested the existence of an alternative transcript.

2.3. Identification of alternative promoters

To map the *Matn2* promoter in transient expression assays, the 2419-bp *Bgl*II-*Sac*I fragment carrying exon 1 and the 5′-flanking region of the gene was shortened gradually at the 5′ end and fused to the luciferase reporter gene (Fig. 2a). Construct M(+56) had as low an activity as the promoterless MIA carrying a fragment from intron A. In NIH-3T3 cells expressing *Matn2* at high level (Piecha et al. 1999), construct M(-39) exhibited 18±0.4% luciferase activity relative to the pGL3-Control Vector carrying the SV40 promoter. Therefore, we concluded that the minimal promoter was located between positions −39 and +56. The relative promoter activity increased to approximately 80% between positions −219 and −517, indicating the presence of a positive control region (Fig. 2a). The promoter and the entire exon 1 were situated in a CpG island. To define the transcription start point more precisely, we performed primer extension analysis using several primers. Two major start sites and several weaker ones were mapped in a GC-rich region in four independent experiments using primers pBr and pCr (Fig. 2b). The region was not preceded by a TATA motif, but carried several putative Sp1 recognition sites characteristic of housekeeping promoters. Furthermore, the mouse RACE clones pCRP207 and pCRP233 as well as 14 mouse EST clones also started between the two major start sites (see later, Fig. 4a). Thus, our primer extension and transient expression data unequivocally defined a housekeeping promoter with multiple initiation sites between positions −39 and +56 relative to the most upstream strong start site.

The human gene showed a high degree of sequence conservation not only within exon 1, but in the promoter region as well. Using the NNPP program, a putative transcription start site designated as +1 in the human sequence was predicted one nt downstream as compared to the upstream major start site of the mouse gene. The human EST entry BF347123 started close to the predicted start point (Fig. 4a). The *MATN2* promoter also lacked a TATA motif and carried putative Sp1 sites in conserved positions.

The difference between the human and mouse cDNA sequences within exon 2 suggested an mRNA heterogeneity arising from alternative splicing or usage of alternative promoters. Sequence analysis did not reveal the occurrence of an alternative acceptor splice site in the corresponding region (see later, Fig. 4b). However, motifs CACCCT and CATTTT were found nearby in the mouse and human sequences, respectively, matching to the CANYYY canonical transcription start site of eukaryotic genes (Corden et al., 1980), and both motifs were preceded by a TATA-like sequence. To address the question whether the gene is also transcribed from an alternative downstream promoter functional only in certain tissues and/or species, we carried out RT-PCR analysis. A set of oligonucleotide primers was designed to investigate how far into the 5′ direction the transcribed region protrudes (Table 1 and Fig. 3a). Selecting reverse primers from exon 3 and forward primers from exon 2B (pIn) or further upstream (pHn and pGn), we detected

Table 2
Exon–intron organization of the mouse and human genes for matrilin-2

Species	Exon	Size (bp)	5′ Splice site	Intron	Size (kb)	3′ Splice site
Mouse	1(5′ UTR)	238	CAGgtgagcgccg	A	9.0[a]	ttgattatagCTG
Human	1	215	CAGgtgagcgcgg	A	18.787	tttgtcacagCCT
Mouse	2A(5′ UTR)	57	TAG	–	–	CTG
Human	2A	122	CAG	–	–	CCT
Mouse	2B(5′ UTR+	165	TGGgtgagtgaga	B	>17.0[a]	ctttccccagAGA
Human	2B sig.pep.)	168	TGGgtgagtggtg	B	42.710	ctttccccagAGA
Mouse	3(vWFA1)	570	GCAgtaagtctgt	C	>11.2[a]	ccctttgcagCAG
Human	3	570	GCAgtaagtcctg	C	10.254	tccctttcagCGG
Mouse	4(EGF1)	123	GAAgtaaggccac	D	>8.0[a]	tttgtctcagTCC
Human	4	123	GAAgtaagattgc	D	19.508	tttgcctcagTCC
Mouse	5(EGF2)	123	CCGgtaggtatct	E	12.0[a]	ttttcttcagCTG
Human	5	123	TGGgtgagtatcc	E	17.355	ttctctccagCTG
Mouse	6(EGF3)	123	CAAgtaagttaca	F	>8.0[a]	ttctttccagAGA
Human	6	123	CAAgtaagttaca	F	15.471	ttcttgccagAGA
Mouse	7(EGF4)	123	GAAgtaagtaacc	G	3.5[a]	ctctccttagGGA
Human	7	123	GAAgtaattccgt	G	9.058	ttcccctcagGGA
Mouse	8(EGF5)	123	GCCgtgagtgtgc	H	7.5[a]	accattgcagGGG
Human	8	123	GCCgtgagtgtac	H	3.321	gaaaatgcagGAG
Mouse	9(EGF6)	123	CCAgtgagttccc	I	0.240	ggtctttcagGGG
Human	9	123	CCCgtgagtccct	I	0.251	ggttttgcagGGG
Mouse	10(EGF7)	123	CAAgtgagtttca	J	>8.0[a]	ttctaactagAAC
Human	10	123	CAAgtaagtgtct	J	8.938	tgattctcagAAT
Mouse	11(EGF8)	123	GAAgtaagtttac	K	1.3[a]	ctctcctcagGGA
Human	11	123	GAAgtaagtttgt	K	1.331	ctgtcttcagGGA
Mouse	12(EGF9)	123	GGAgtaagtagct	L	2.3[a]	ttttccctagGGA
Human	12	123	GAAgtaagtagcc	L	3.088	ttttcctcagGGA
Mouse	13(EGF10)	123	AGAgtaagtgacc	M	2.3[a]	attcctatagGAT
Human	13	123	AGAgtaagtgatc	M	6.088	gttcatatagAAT
Mouse	14(vWFA2-1)	414	ATGgtaatgggat	N	3.0[a]	tgttgcttagGTA
Human	14	414	ATGgtaatatggg	N	2.631	tgcaccctagGTA
Mouse	15(vWFA2-2)	153	AAGgtattataga	O	0.989	ttccattcagCTC
Human	15	153	AAGgtactatcgt	O	1.631	ttctgctcagCTC
Mouse	16(U/1)	72	CAGgtgagtctta	P	0.317	ctcttcacagAAC
Human	16	72	CAGgtacagtttt	P	0.724	ctctttacagAAT
Mouse	17(U/2)	135	CAGgtaattccaa	Q	0.318	gctttctcagGAA
Human	17	135	CAGgtaattccaa	Q	0.384	gctttctcagGAA
Mouse	18(CC/1)	99	GCTatatccttt	R	2.1[a]	tgagatttacTAG
Human	18	99	GCTatatccttt	R	1.997	tgagatttacTAG
Mouse	19(CC/2+	450				
Human	19 3′ UTR)	500				
Consensus sequence[b]			KAGgtragt			yag G

[a] Intron size was estimated with restriction mapping and PCR.
[b] Consensus for U2-type GT-AG introns (Sharp and Burge, 1997). R, purine; Y, pyrimidine; K, A or C; U, unique sequence; CC, coiled coil.

downstream promoter activity in RNA samples prepared from mouse embryos at E7.5 and E11.5 (data not shown). In mouse primary embryo fibroblast samples, RT-PCR product of expected size and sequence was also generated with pHn starting 5 nt downstream of the putative start site, but no fragment was amplified using pGn selected close upstream of the CACCCT motif (Fig. 3b and Fig. 4b). Therefore, we designated A as the initiating nucleotide for the downstream promoter (P_d). Computer analysis using the NNPP program also placed the transcription start site within the hexanucleotide motif and predicted a promoter within the region, in congruence with the hypothesis that GAAAAAT, a non-canonical TATA box located 27 bp upstream can function as a promoter of *Matn2* (Fig. 4b). A similar motif drives the transcription of *Rps16* (Wagner and Perry, 1985). Detection of artifacts was excluded, as no fragments appeared in the control PCR assays performed without reverse transcription in this and all other experiments described in this paper.

Samples from various adult tissues and mouse cell lines were tested by RT-PCR to reveal the tissue-specificity of P_d. The activity of P_d remained below a detectable level in adult tissues, as well as in C2/7 myoblasts and SVEC endothelial cells, which expressed the gene at a high level from the upstream promoter (P_u) (Fig. 3b–d). However, P_d was functional in the NIH-3T3 embryo fibroblast cell line (Fig. 3d).

Table 3
U12-type AT-AC introns in the matrilin gene family

Genes	5′ Splice site	Branch site	3′ Splice site
Matrilin-1/CMP			
Mouse Y13902[a]	AGCatatccttt	gcccttaactcc	tacTGG
Human M55682[a]	AACatatccctt	ctccttaactct	cacTGG
Chick X12352-3[a]	AATatatccttt	ctccttaactct	cacTGG
Matrilin-2			
Mouse AF358843[a] AF358844[a]	GCTatatccttt	ttccttaatttg	tacTAG
Human AC019236[a]	GCTatatccttt	ttccttaatttg	tacTAG
Matrilin-3			
Mouse AJ242935[a]	AACatatccttt	ctccttaaccgc	cacTTG
Human AC079145[a]	ACCatatccttt	ggccttaacaac	cacTTG
Matrilin-4			
Mouse AJ291700[a]	ACCatatccttt	ttccttaaccgc	cacTGG
Human AL021578[a]	ACCatatccttt	ggccttaacatc	cacTGG
Consensus[b]	atatccttt	ttccttracycy	yac

[a] GenBank Accession Number.
[b] Consensus for U12-type AT-AC introns (Sharp and Burge, 1997).

In similar experiments, we confirmed that P_d is active in the human WI-26 lung fibroblast and HEp-2 epithelial cell lines, but undetectable in a primary fibroblast culture obtained from adult skin (NHSF) (Fig. 3e). Using forward primers pRn, pSn, pTn and pVn, we mapped the start point within a 14-nt interval between pSn and pTn, which includes the putative CATTTT start site. We designated A of this motif as the initiating nucleotide for P_d of *MATN2* in Fig. 4b. 34 bp further upstream a TATA-like motif (ACTTAA) was found (Fig. 4b), which is an active promoter element of the mouse and rat link protein gene (Deák et al., 1999a). As we mapped the human start site for P_d further upstream than in mouse, the length of the untranslated exon 2A differs by 65 nt between the two species (Table 2).

The human and the mouse sequences showed high degree of similarity even upstream of exon 2A (Fig. 4b). We searched for the presence of putative binding sites of known transcription factors in this region, and found several motifs in conserved position in both species for PRRX2, a mesenchyme-specific, paired-related homeobox protein.

Thus, we conclude that both *MATN2* and *Matn2* are transcribed from two alternative promoters (Fig. 4). The upstream housekeeping type promoter is functional in fibroblasts and in a great variety of other cell types expressing the gene. However, the downstream TATA-like promoter has a restricted tissue-specificity, being active only in embryo fibroblasts and certain cell lines.

2.4. Chromosome location of Matn2

Single strand conformation polymorphisms (SSCP) analysis was used as previously described (Brady et al., 1997) to map *Matn2*. Primers were designed to find

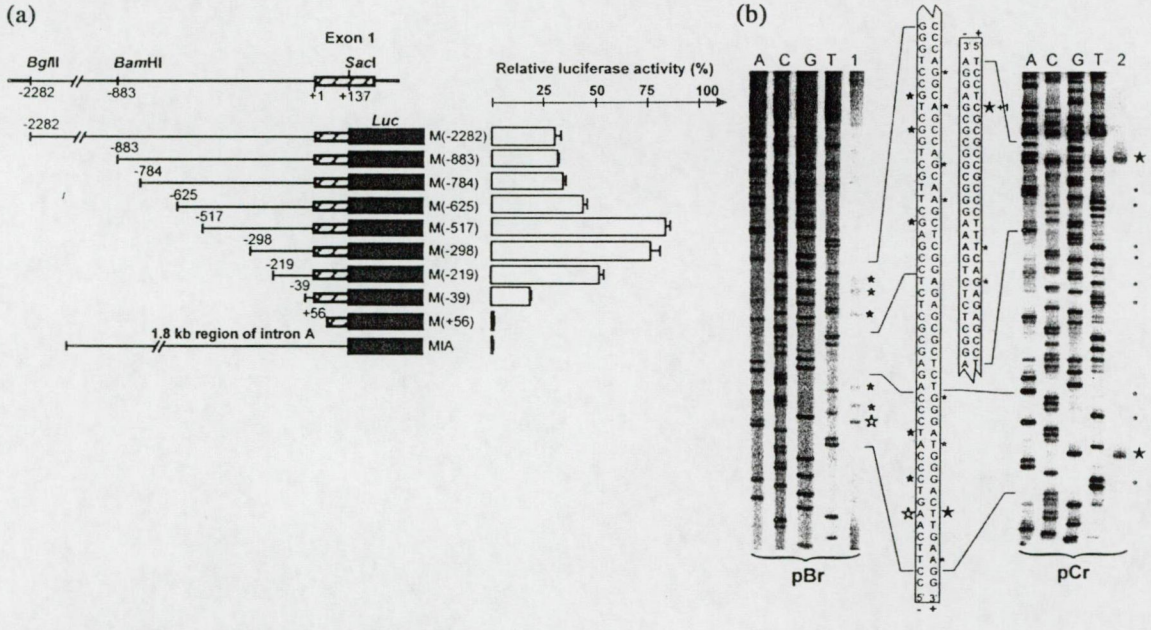

Fig. 2. Mapping of the upstream promoter and transcription start sites of *Matn2*. (a) Functional analysis of the promoter region. Left panel depicts the schematic drawing of *Matn2* promoter-luciferase reporter gene fusion constructs. Positions are indicated in bp with reference to the start site of the longest transcript defined in Fig. 2b. Plasmids were transfected into NIH-3T3 cells. MIA carrying a promoterless intronic fragment served as a negative control. Luciferase activities are expressed in percentage of that of pGL3-Control vector (SV40 promoter) transfected in parallel plates. Data in the right panel represent means ± S.E. (b) Mapping of the transcription start points in primer extension experiments. Lanes 1 and 2 include primer extension products made on NIH-3T3 RNA as a template using primers (Table 1) indicated below. The products were run along with a sequencing ladder generated from the same primer. Start sites determined using primers pBr and pCr are indicated by open and closed asterisks, respectively, at both sides on the sequence.

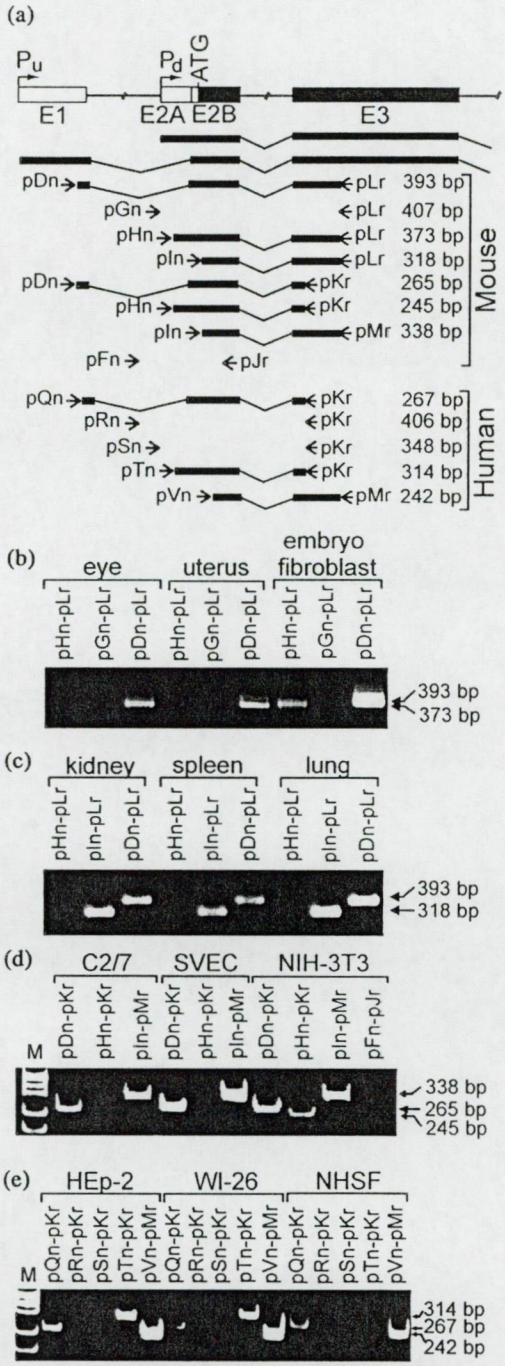

Fig. 3. Identification and tissue specificity of the downstream promoter of *Matn2* and *MATN2* by RT-PCR analysis. (a) Schematic drawing of the PCR primers (Table 1) and products with respect to the positions of exons and the two promoters. Open bars indicate the UTR. (b–d) RT-PCR analysis of RNA samples derived from mouse tissues, primary cell culture and permanent mouse cell lines. (e) RT-PCR analysis of RNA samples derived from human permanent cell lines (HEp-2 and WI-26) and primary culture of adult skin fibroblasts (NHSF). RT-PCR products were electrophoresed in agarose (b and c) and polyacrylamide (d and e) gels. M, *Msp*I digest of pUC12.

SSCP between inbred mouse strains in the introns between exon 15 and 18 of *Matn2*. The BSS interspecific backcross was genotyped and the allele distribution pattern analyzed using the Map Manager program (Fig. 5). *Matn2* was found to map to chromosome 15 with a LOD likelihood score of 28. No recombinants were found in 94 progeny between *Matn2* and *Sema5a*. The position of *Matn2* with respect to flanking microsatellite markers is: *D15Mit10, D15Mit13* - 4.26±2.08 cM — *Sema5a, Matn2* - 18.08±3.97 cM - *D15Mit3*.

3. Discussion

We reported previously the molecular cloning of matrilin-2, the second member of the matrilin family of filament-forming proteins implicated in the organization of the ECM (Deák et al., 1997, 1999b). The family consists of four members: matrilin-1 and -3 forming homo- and heterooligomers in skeletal elements, and matrilin-2 and -4 functioning in many tissues (Deák et al., 1999b). Matrilin-1 was proposed to serve as an adapter protein in the cartilaginous ECM, because it can interact both with type II collagen and aggrecan (Winterbottom et al., 1992; Hauser et al., 1996). So far, mutations have been identified only for matrilin-3 causing one form of MED, a frequently occurring skeletal disease (Chapman et al., 2001). Based on their similar domain structures, including the presence of one or two vWFA domains and the observation that each cell type expresses one or more matrilins, the other matrilins are also likely to perform an important adapter function in the ECM. To facilitate the identification of mutations in other matrilin genes and to promote functional studies in transgenic mice, here we describe the comparative analysis of the genomic organization and chromosome location of the mouse and human genes for matrilin-2, the largest member of the family.

SSCP analysis was used to localize *Matn2* to mouse chromosome 15, linked to the genes *Trhr* and *Sntb1*. The human orthologues of these genes have been mapped to 8q23-24 (Ahn et al., 1994; Morrison et al., 1994). We formerly mapped *MATN2* by fluorescence in situ hybridization at chromosome position 8q22 (Muratoglu et al., 2000). Therefore, all three mouse genes were mapped to the region synthenic to human chromosome 8q22-24. *Sema5a* and *ank* are also closely linked to *Matn2* on the mouse chromosome 15 (Sweet and Green, 1981). As the *ank* mutation causes progressive ankylosis, we performed PCR analysis on DNA isolated from *ank/ank* mice to check the possibility that this phenotype is due to a mutation in *Matn2*. Sequence analysis of the PCR products covering the entire coding region and all exon–intron borders of *Matn2*, however, revealed no alterations compared to the wild type

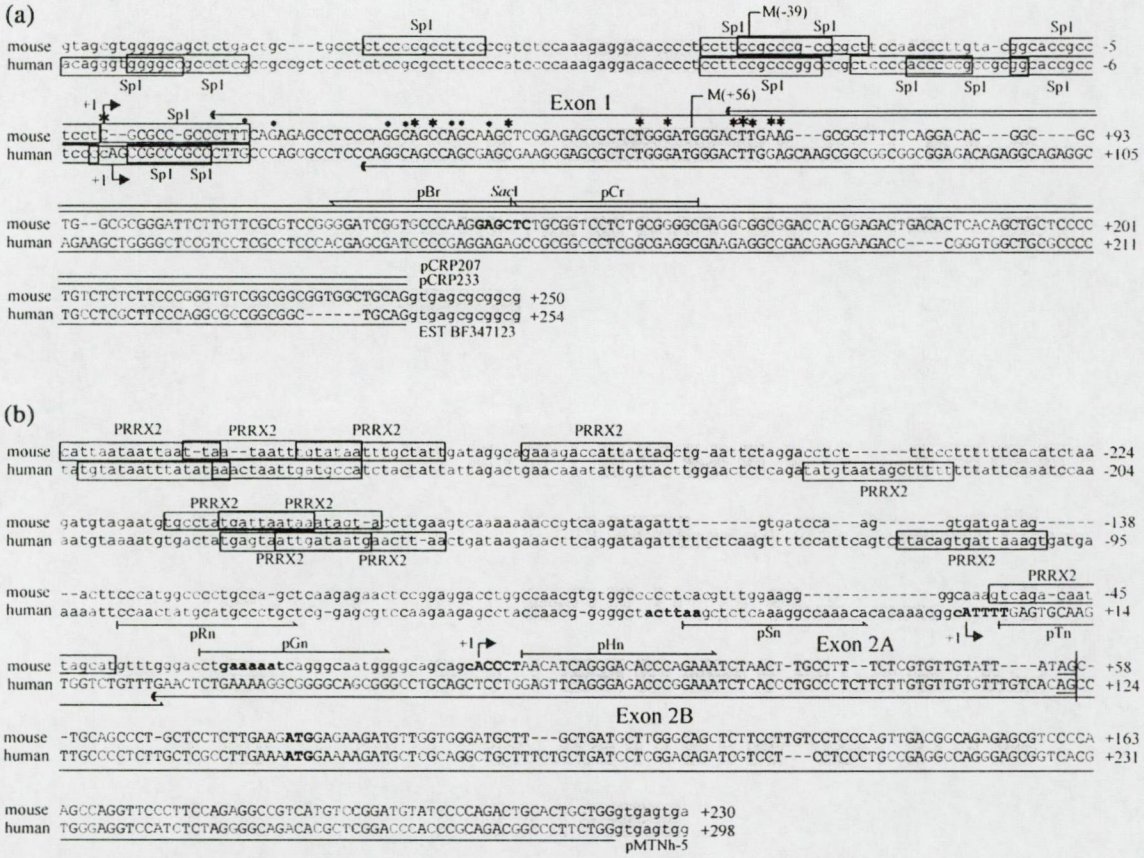

Fig. 4. Comparison of the promoter regions of *Matn2* and *MATN2*. (a) Alignment of exon 1 and the 5′-flanking sequences. RNA synthesis start points determined in four independent experiments are denoted by asterisks. (b) Nucleotide sequence of exon 2 and the surrounding regions. Translation initiation sites, TATA-like motifs and putative transcription start sites are bold-faced. The highlighted letters indicate matching bases. Putative binding sites for transcription factors Sp1 and PRRX are boxed. Locations of EST and RACE clones and positions of primers used to map the start sites are delineated.

sequence suggesting that matrilin-2 is not causative for progressive ankylosis. While this work was in progress, characterization of mouse and human mutations confirmed that *ank* codes for a multipass transmembrane protein (Ho et al., 2000; Nurnberg et al., 2001). Interestingly, the human orthologues of *ank* and *Sema5a* were assigned to another synthenic region at 5p15.2-p14.1 (Nurnberg et al., 2001). The Cohen syndrome characterized by face, oral, ocular and limb deformities, hypotonia and mental deficiency, however, was mapped at human chromosome 8q22-23 (Cohen et al., 1973). Further analysis will reveal, whether mutations in *MATN2* cause this disease.

Both *Matn2* and *MATN2* are very large, >100 kb and 167.167 kb in length, respectively, and consist of 19 exons. The genomic organization of the two genes is identical to each other and shows similarities to other matrilin genes. In all the matrilin genes, phase I introns are located at the domain borders, lining up with the hypothesis that exon duplication and exon shuffling within phase I introns played an important role in the evolution of the matrilin family. The most remarkable common feature of all four matrilin genes is that a phase I, U-12-type AT-AC intron separates in a strictly conserved position the two exons for the coiled coil domain (Muratoglu et al., 2000 and this work). This reflects that the AT-AC intron was present in the common ancestor of matrilin genes. Furthermore, this conservation strongly indicates that the minor spliceosome, which occurs in the cells in a 100-fold lower amount than the major spliceosome (Tarn and Steitz, 1996), may have an important regulatory role in the coordinated expression of the matrilin genes.

Contrary to *Matn2*, the other matrilin genes are rather compact (Kiss et al., 1989; Wagener et al., 1998, 2000, 2001). Matrilin-2 differs from the other matrilins in the presence of the unique segment and the large number of EGF modules (Deák et al., 1997, 1999b). In the closely related human and mouse matrilin-4 genes, alternative splicing leads to the excision of exons encoding the EGF and the first vWFA domains (Wagener et al., 1998, 2001). In the protein coding region of *MATN2*,

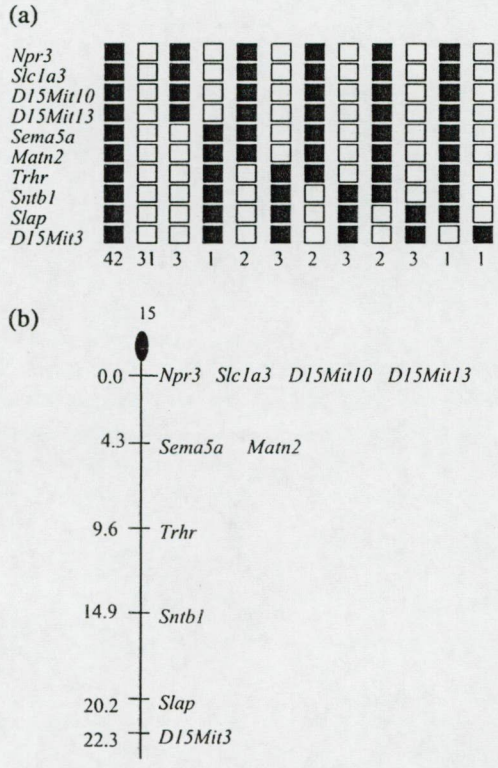

Fig. 5. Chromosomal location of *Matn2*. (a) Haplotype of the region surrounding *Matn2* on chromosome 15 in 94 progeny of the BSS cross. Filled boxes represent the C57Bl6/J allele, open boxes represent *Mus musculus spretus*. (b) Genetic map of the region.

alternative splicing affects only the unique segment, but no variations in the number of EGF and vWFA modules were observed (Muratoglu et al., 2000). On the other hand, two alternative promoters control the broad tissue-specific expression of both *Matn2* and *MATN2*. While a single promoter drives the transcription from *Matn1* and *Matn3* (Kiss et al., 1989; Wagener et al., 2000), the broad tissue-specificity of *Matn4* is also achieved by the usage of alternative promoters (Wagener et al., 2001). Contrary to *Matn4*, however, the upstream promoter of *Matn2* and *MATN2* works as a major promoter in most tissues, and the downstream promoter has a very narrow tissue-specificity.

Data presented here indicate that P_u, which exhibits the characteristics of housekeeping promoters, is used much more frequently than P_d, especially in *Matn2*. Thus, active transcription was observed from P_d in all the samples, but transcription from P_d was below the level of detection in any of nine distinct adult mouse organs tested (Fig. 3b,c and data not shown). On the other hand, in samples from whole embryos, primary fibroblasts derived from E14.5 embryos and the NIH-3T3 embryo fibroblast cell line, we detected transcription from P_d by RT-PCR. Only P_u, but not P_d, was active in SV40-transformed lymphoid vascular endothelial cells (SVEC) and C2/7 myotubes. Previously, *Matn2* expression was found by RT-PCR, in situ and Northern hybridization in all mouse, rat and human samples of fibroblastic, smooth muscle, epithelial, endothelial and Schwann cell origin (Piecha et al. 1999; Muratoglu et al., 2000). In fact, there was no RNA sample studied where *Matn2* expression was below the detectability threshold. Therefore, we may conclude that there is a basic level of transcription of *Matn2* in the various cell types, most probably from the P_u promoter. The Sp1-binding motifs found in multiple copies in both species may have a role in the ubiquitous activity of P_u, as Sp1 was demonstrated to contribute to the activity of many genes with broad expression pattern (Philipsen and Suske, 1999).

On the other hand, P_d seems to be regulated more strictly and have a preference in mouse embryo for fibroblasts. This promoter has a TATA-like motif, and contains several putative binding sites for paired related homeobox-2 (PRRX2 or S8). Interestingly, potential 8-bp motifs recognized by the same transcription factor precede the promoter of *Matn3* and the weaker upstream promoter of *Matn4*. This observation raises the possibility that PRRX2/S8 may be an important regulator of matrilin genes coordinating their expression. The potential role of PRRX2/S8 in the control of *Matn2* is supported by the remarkable overlap in the expression pattern of the two genes. A transcript of the *Prrx2* gene was relatively abundant in NIH-3T3 fibroblasts. In pluripotent embryonic carcinoma and embryonic stem cells, expression could be induced upon differentiation by different means, but among terminally differentiated cells, only fibroblasts expressed *Prrx2* (de Jong and Meijlink, 1993). In mouse embryos, the *Prrx2* mRNA was accumulated in cranial mesenchyme, limb buds, axial mesoderm, generally in regions which develop into connective tissue (Leussink et al., 1995). Previously, we observed *Matn2* expression by in situ hybridization in the cells of dense and loose connective tissue (Piecha et al., 1999). Furthermore, the *Prrx2* expression pattern shows positive correlation with deposition of matrilin-2 in mouse limbs at perinatal ages. Both gave the strongest signal in tendon, perichondrium, periosteum and ligaments, plus the reticular layer of dermis (Piecha et al., 1999; Leussink et al., 1995). Mice carrying double mutation in *Prrx2* and the closely related *Prrx1* also exhibited abnormalities in epitheliomesenchymal interactions in the limbs, aortic arch and inner ear (ten Berge et al., 1998). To sum up, given the significant overlap between the expression domains of *Matn2* and *Prrx2*, the PRRX2 transcription factor may contribute to the fibroblast-specific expression of *Matn2*. The frequent occurrence of PRRX2 binding sites upstream of P_d also supports that the fibroblast-specific expression of *Matn2* is regulated partly by PRRX2.

4. Materials and methods

4.1. Isolation and analysis of genomic clones

Genomic clones encoding matrilin-2 were obtained from the mouse 129/Sv strain using different methods. First, seven different clones were isolated during the screening of a mouse 129/Sv genomic library (Stratagene) made in λFixII vector with matrilin-2 cDNA probes (Deák et al., 1997) as described previously (Kiss et al., 1989). The genomic clone pEx1 carrying exon 1 was made by inverse PCR (Ochman et al., 1988). Briefly, for creating sufficient template, EcoRI digested mouse 129/Sv genomic DNA was religated at a final concentration of 20 ng/μl. Two pairs of nested primers, pAr/pEn and pBr/pDn (Table 1) pointing out of the exon 1 sequence were used for PCR amplification. To isolate the genomic region covering the missing promoter and exon 4, the mouse 129/Sv genomic PAC library RPCI21 (Osoegawa et al., 2000) was screened with pEx1 as a hybridization probe. Out of the six positive PACs obtained from the Human Genome Mapping Project Resource Centre (UK), PAC477-O13 was characterized further. Restriction endonuclease mapping and Southern hybridization of phage DNA and subclones were performed according to standard methods. Sizes of some of the introns were determined by PCR analysis using exon-specific primers. Nucleotide sequences were determined on both strands of purified phage DNA or suitable fragments subcloned into pBluescript using an ABI373 automated DNA sequencer (Applied Biosystems), a Dye Terminator Cycle Sequencing Kit (Perkin–Elmer/Cetus) and T7-, T3-, or gene-specific primers.

Cloning of full-length human matrilin-2 cDNA and 3′ genomic region (pD280 and pD281) were reported recently (Muratoglu et al., 2000). Additional genomic and EST sequence data were also obtained from the National Center for Biotechnology Information Database (http://www.ncbi.nlm.nih.gov/). Sequence similarity search was performed with the BLAST program (Altschul et al., 1997). DNA sequences were analyzed using utility software available at 'Search launcher' of the Human Genome Sequencing Center, Baylor College of Medicine (http://searchlauncher.bcm.tmc.edu/). Exons, transcription factor binding sites, promoters and CpG islands were predicted using programs GENSCAN (http:/CCR-081.mit.edu/GENSCAN.html), Matinspector/TRANSFAC (http://www.gsf.de/cgi-bin/matsearch.pl), NNPP (http://www.fruitfly.org/seq-tools/promoter.html) and CpG Plot (http://www.ebi.ac.uk/emboss/cpgplot/), respectively.

4.2. Construction of promoter/reporter plasmids

A nested set of mouse promoter fragments was fused to the luciferase reporter gene in several steps. First, the 2419-bp *Bgl*II-*Sac*I and the 1020-bp *Bam*HI-*Sac*I promoter fragments of *Matn2* were ligated into the *Bgl*II site of pGL3-Basic vector (Promega Corp.) to yield constructs M(-2282) and M(-883), respectively. To generate a nested 5′ deletion set, the promoter fragment of M(-883) was shortened using the ExoIII/S1 nuclease kit (Promega Corp.). A 1.8-kb *Hin*dIII fragment from intron A was also inserted into the same vector to obtain the promoterless control plasmid MIA. The orientation and structure of all constructs were confirmed by restriction mapping and sequencing.

4.3. Cell culture and transfection

The NIH-3T3 mouse embryonic fibroblast cell line and the C2/7 myotubes were obtained and maintained as described (Piecha et al., 1999). Human epithelial HEp-2 and fetal lung fibroblast WI-26 cell lines were obtained from the American Type Culture Collection and cultivated as suggested by the supplier. Primary fibroblasts were isolated from E14 mouse embryos and human skin biopsies (NHSF) by tryptic digestion and cultured in DMEM supplemented with 10% fetal calf serum (Life Technologies).

With the calcium phosphate coprecipitation method, 1.5×10^6 NIH-3T3 cells were transfected as described (Szabó et al., 1995), and the luciferase activity was measured using reagents and protocols from Promega Corp. To normalize for the transfection efficiency, 5 μg of pTKCAT DNA was used as an internal control. Parallel plates were transfected with pGL3-Control Vector (Promega Corp.) and the promoterless plasmid MIA as positive and negative controls, respectively. Duplicate plates were made for each DNA and the experiments were repeated three times with at least two independent plasmid preparations. Promoter activities were given in percentage of that of pGL3-Control Vector.

4.4. RNA purification and mapping of the transcription start sites

RNA was prepared from guanidium thiocyanate extracts of tissue samples or cultured cells as described (Deák et al., 1997). For RT-PCR, total RNA aliquots were treated with RNase-free DNase (Roche Molecular Biochemicals). Of total RNA, 0.7 μg was reverse transcribed in 20 μl with 80 U of M-MuLV reverse transcriptase (Life Technologies) using gene-specific primers. In 25-μl final volume at 95 °C, 2 μl of the cDNA was heated for 3 min and the appropriate fragments were amplified by AmpliTaq DNA polymerase (Perkin–Elmer/Cetus) during 40 cycles (30 s at 95 °C, 30 s at 57 °C and 1 min at 72 °C).

RNA from NIH-3T3 cells was annealed to biotinylated oligo(dT), anchored to streptavidin-coated paramagnetic beads (Amersham Pharmacia Biotech) and eluted

with distilled water to isolate poly(A)$^+$ RNA. For primer extensions, 0.1–0.5 pmoles of end-labeled primers pBr or pCr were annealed with up to 30 μg of total RNA or 2 μg of poly(A)$^+$ RNA, and elongated with 200 units of M-MuLV reverse transcriptase.

4.5. Chromosome localization

To test for SSCPs between mouse strains as described previously (Brady et al., 1997), primers were designed to amplify a region corresponding to intronic sequences of *Matn2*. The primer pairs pNn/pOr and pNn/pPr identified a polymorphism between *M. m. musculus* C57BL/6J and *M. m. spretus*. Allele distribution was determined in the BSS panel using the Map Manager Program (Manly, 1993) as described (Deák et al., 1999a).

Acknowledgments

We thank Katalin Illés, Anikó Simon and Irén Fekete for excellent technical assistance and Mária Tóth for the artwork. This work was supported by grants OTKA T022224, T034399, C0038 and M027770 to I.K.; and grant OTKA T029157 to F.D. from the Hungarian National Scientific Research Foundation; and a grant from the Swedish Medical Research Council to A.A. This publication was supported by the Rollin D. Hotchkiss Foundation.

References

Ahn, A.H., Yoshida, M., Anderson, M.S., et al., 1994. Cloning of human basic A1, a distinct 59-kDa dystrophin-associated protein encoded on chromosome 8q23-24. Proc. Nat. Acad. Sci. USA 91, 4446–4450.

Altschul, S.F., Madden, T.L., Schäffer, A.A., et al., 1997. Gapped BLAST and PSI-BLAST: a new generation of protein database search programs. Nucleic Acids Res. 25, 3389–3402.

Aszódi, A., Bateman, J.F., Hirsch, E., et al., 1999. Normal skeletal development of mice lacking matrilin 1: redundant function of matrilins in cartilage? Mol. Cell. Biol. 19, 7841–7845.

Brady, K.P., Rowe, L.B., Her, H., et al., 1997. Genetic mapping of 262 loci derived from expressed sequences in a murine interspecific cross using single-strand conformational polymorphism (SSCP) analysis. Genome Res. 7, 1085–1093.

Chapman, K.L., Mortler, G.R., Chapman, K., Loughlin, J., Grant, M.E., Briggs, M.D., 2001. Mutations in the region encoding the von Willebrand factor A domain of matrilin-3 are associated with multiple epiphyseal dysplasia. Nat. Genet. 28, 393–396.

Chen, Q., Zhang, Y., Johnson, D.M., Goetinck, P.F., 1999. Assembly of a novel cartilage matrix protein filamentous network: molecular basis of differential requirement of von Willebrand factor A domains. Mol. Biol. Cell 10, 2149–2162.

Cohen, M.M., Hall, B.D., Smith, D.W., Graham, C.B., Lampert, K.J., 1973. A new syndrome with hypotonia, obesity, mental deficiency, and facial, oral, ocular and limb anomalies. J. Pediatr. 83, 280–284.

Corden, J., Wasylyk, B., Buchwalder, A., Sassone-Corsi, P., Kedinger, C., Chambon, P., 1980. Promoter sequences of eukaryotic protein-coding genes. Science 209, 1406–1414.

de Jong, R., Meijlink, F., 1993. The homeobox gene S8: mesoderm-specific expression in presomite embryos and in cells cultured in vitro and modulation in differentiating pluripotent cells. Dev. Biol. 157, 133–146.

Deák, F., Mátés, L., Krysan, K., et al., 1999. Characterization and chromosome location of the mouse link protein gene (Crtl1). Cytogenet. Cell Genet. 87, 75–79.

Deák, F., Piecha, D., Bachrati, C., Paulsson, M., Kiss, I., 1997. Primary structure and expression of matrilin-2, the closest relative of cartilage matrix protein within the von Willebrand factor type A module superfamily. J. Biol. Chem. 272, 9268–9274.

Deák, F., Wagener, R., Kiss, I., Paulsson, M., 1999. The matrilins: a novel family of oligomeric extracellular matrix proteins. Matrix Biol. 18, 55–64.

Hauser, N., Paulsson, M., Heinegård, D., Mörgelin, M., 1996. Interaction of cartilage matrix protein with aggrecan: Increased covalent cross-linking with tissue maturation. J. Biol. Chem. 217, 32247–32252.

Ho, A.M., Johnson, M.D., Kingsley, D.M., 2000. Role of the mouse ank gene in control of tissue calcification and arthritis. Science 289, 265–270.

Huang, X., Birk, D.E., Goetinck, P.F., 1999. Mice lacking matrilin-1 (cartilage matrix protein) have alterations in type II collagen fibrillogenesis and fibril organization. Dev. Dyn. 216, 434–441.

Kiss, I., Deák, F., Holloway, R.G., et al., 1989. Structure of the gene for cartilage matrix protein, a modular protein of the extracellular matrix. J. Biol. Chem. 264, 8126–8134.

Klatt, A., Nitsche, D.P., Kobbe, B., Macht, M., Paulsson, M., Wagener, R., 2001. Molecular structure, processing and tissue distribution of matrilin-4. J. Biol. Chem. 276, 17267–17275.

Klatt, A., Nitsche, D.P., Kobbe, B., Mörgelin, M., Paulsson, M., Wagener, R., 2000. Molecular structure and tissue distribution of matrilin-3, a filament-forming extracellular matrix protein expressed during skeletal development. J. Biol. Chem. 275, 3999–4006.

Lee, J.-O., Rieu, P., Arnaout, M.A., Liddington, R., 1995. Crystal structure of the A domain from the a subunit of integrin CR3 (CD11b/CD18). Cell 80, 631–638.

Leussink, B., Brouwer, A., el Khattabi, M., et al., 1995. Expression patterns of the paired-related homeobox genes MHox/Prx1 and S8/Prx2 suggest roles in development of the heart and the forebrain. Mech. Dev. 52, 51–64.

Makihira, S., Yan, W., Ohno, S., et al., 1999. Enhancement of cell adhesion and spreading by a cartilage-specific noncollagenous protein, cartilage matrix protein (CMP/Matrilin-1), via integrin alpha1beta1. J. Biol. Chem. 274, 11417–11423.

Manly, K.F., 1993. A Macintosh program for storage and analysis of experimental genetic mapping data. Mamm. Genome 4, 303–313.

Morrison, N., Duthie, S.M., Boyd, E., Eidne, K.A., Connor, J.M., 1994. Assignment of the gene encoding the human thyrotropin-releasing hormone receptor to 8q23 by fluorescence in situ hybridization. Hum. Genet. 93, 716–718.

Muratoglu, S., Krysan, K., Balázs, M., et al., 2000. Primary structure of human matrilin-2, chromosome location of the MATN2 gene and conservation of an AT-AC intron in matrilin genes. Cytogenet. Cell Genet. 90, 323–327.

Nurnberg, P., Thiele, H., Chandler, D., et al., 2001. Heterozygous mutations in ANKH, the human ortholog of the mouse progressive ankylosis gene, result in craniometaphyseal dysplasia. Nat. Genet. 28, 37–41.

Ochman, H., Gerber, A.S., Hartl, D.L., 1988. Genetic applications of an inverse polymerase chain reaction. Genetics 120, 621–623.

Osoegawa, K., Mammoser, A.G., Wu, C., et al., 2000. Bacterial artificial chromosome libraries for mouse sequencing and functional analysis. Genome Res. 10, 116–128.

Philipsen, S., Suske, G., 1999. A tale of three fingers: the family of mammalian Sp/XKLF transcription factors. Nucleic Acids Res. 27, 2991–3000.

Piecha, D., Muratoglu, S., Mörgelin, M., et al., 1999. Matrilin-2, a large, oligomeric matrix protein, is expressed by a great variety of cells and forms fibrillar networks. J. Biol. Chem. 274, 13353–13361.

Sharp, P.A., Burge, C.B., 1997. Classification of introns: U2-type or U12-type. Cell 91, 875–879.

Sweet, H.O., Green, M.C., 1981. Progressive ankylosis, a new skeletal mutation in the mouse. J. Hered. 72, 87–93.

Szabó, P., Moitra, J., Rencendorj, A., Rákhely, G., Rauch, T., Kiss, I., 1995. Identification of a nuclear factor-I family protein-binding site in the silencer region of the cartilage matrix protein gene. J. Biol. Chem. 270, 10212–10221.

Tarn, W.Y., Steitz, J.A., 1996. A novel spliceosome containing U11, U12 and U5 snRNPs excises a minor class (AT-AC) intron in vitro. Cell 84, 801–811.

ten Berge, D., Brouwer, A., Korving, J., Martin, J.F., Meijlink, F., 1998. Prx1 and Prx2 in skeletogenesis: roles in the craniofacial region, inner ear and limbs. Development 125, 3831–3842.

Wagener, R., Kobbe, B., Aszódi, A., Aeschlimann, D., Paulsson, M., 2001. Characterization of the mouse matrilin-4 gene: A 5′ antiparallel overlap with the gene encoding the transcription factor RBP-L. Genomics 76, doi:10.1006/geno.2001.6589. Genomics 76, 89–98.

Wagener, R., Kobbe, B., Aszódi, A., Liu, Z., Beier, D., Paulsson, M., 2000. Structure and mapping of the mouse matrilin-3 gene (Matn3), a member of a gene family containing a U12-type AT-AC intron. Mamm. Genome 11, 85–90.

Wagener, R., Kobbe, B., Paulsson, M., 1998. Genomic organisation, alternative splicing and primary structure of human matrilin-4. FEBS Lett. 438, 165–170.

Wagner, M., Perry, R.P., 1985. Characterization of the multigene family encoding the mouse S16 ribosomal protein: strategy for distinguishing an expressed gene from its processed pseudogene counterparts by an analysis of total genomic DNA. Mol. Cell. Biol. 5, 3560–3576.

Winterbottom, N., Tondravi, M.M., Harrington, T.L., Klier, F.G., Vertel, B.M., Goetinck, P.F., 1992. Cartilage matrix protein is a component of the collagen fibril of cartilage. Dev. Dyn. 193, 266–276.

P3

ARTICLE IN PRESS

Available online at www.sciencedirect.com
SCIENCE DIRECT®

Matrix Biology xx (2004) xxx–xxx

MATRIX BIOLOGY

www.elsevier.com/locate/matbio

Mice lacking the extracellular matrix adaptor protein matrilin-2 develop without obvious abnormalities

Lajos Mátés[a], Claudia Nicolae[b], Matthias Mörgelin[c], Ferenc Deák[a], Ibolya Kiss[a], Attila Aszódi[b,*]

[a]*Institute of Biochemistry, Biological Research Center of the Hungarian Academy of Sciences, H-6701 Szeged, Hungary*
[b]*Department for Molecular Medicine, Max Planck Institute for Biochemistry, Am Klopferspitz 18A, D-82152 Martinsried, Germany*
[c]*Department of Cell and Molecular Biology, Section of Molecular Pathogenesis, BMC/B14, University of Lund, S-22184 Lund, Sweden*

Received 15 January 2004; received in revised form 28 April 2004; accepted 5 May 2004

Abstract

Matrilins are putative adaptor proteins of the extracellular matrix (ECM) which can form both collagen-dependent and collagen-independent filamentous networks. While all known matrilins (matrilin-1, -2, -3, and -4) are expressed in cartilage, only matrilin-2 and matrilin-4 are abundant in non-skeletal tissues. To clarify the biological role of matrilin-2, we have developed a matrilin-2-deficient mouse strain. Matrilin-2 null mice show no gross abnormalities during embryonic or adult development, are fertile, and have a normal lifespan. Histological and ultrastructural analyses indicate apparently normal structure of all organs and tissues where matrilin-2 is expressed. Although matrilin-2 co-localizes with matrilin-4 in many tissues, Northern hybridization, semiquantitative RT-PCR, immunohistochemistry and biochemical analysis reveal no significant alteration in the steady-state level of matrilin-4 expression in homozygous mutant mice. Immunostaining of wild-type and mutant skin samples indicate no detectable differences in the expression and deposition of matrilin-2 binding partners including collagen I, laminin-nidogen complexes, fibrillin-2 and fibronectin. In addition, electron microscopy reveals an intact basement membrane at the epidermal–dermal junction and normal organization of the dermal collagen fibrils in mutant skin. These data suggest that either matrilin-2 and matrilin-2-mediated matrix–matrix interactions are dispensable for proper ECM assembly and function, or that they are efficiently compensated by other matrix components including wild-type levels of matrilin-4.

Keywords: Extracellular matrix; Matrilin; Cartilage; Skin

1. Introduction

Extracellular matrices (ECMs) are highly organized structures that perform diverse roles during development, tumorigenesis, and tissue repair. The cell modifying actions of ECM components are partially mediated by intracellular signals induced by ECM ligands binding cellular receptors. Further interactions between different matrix proteins are essential for proper ECM assembly and play a crucial role in maintaining the structural integrity and physical properties of connective tissues. The multifunctional nature of ECM components is highlighted by the relatively limited set of modules found to comprise most of these proteins.

The matrilins are a family of ECM proteins, which share similar modular structure. The family consists of four members (matrilin-1, -2, -3, and -4), each carrying one or two von Willebrand factor A (vWFA)-like modules, a various number of epidermal growth factor (EGF)-like motifs, and a coiled-coil (CC) oligomerization domain (reviewed in Deák et al., 1999). Matrilin-1 and -3 are expressed primarily in cartilage, while matrilin-2 and -4 have a broader tissue distribution. Matrilin-2 is the largest member of the family. Analysis of the mouse and human matrilin-2 cDNA sequences revealed that the precursor protein consists of a putative signal peptide, two vWFA-like domains separated by ten EGF-like motifs, a unique segment not identified in other matrilins, and a CC domain (Deák et al., 1997; Muratoglu et al., 2000). In tissue extracts and cell culture medium, matrilin-2 exists as mono-, di-, tri-, and tetramers, as demonstrated by SDS-PAGE and electron microscopy (Piecha et al., 1999). In addition to forming homotypic oligomers, biochemical and biophysical char-

*Corresponding author. Tel.: +49-89-8578-2849; fax: +49-89-8578-2422.
E-mail address: aszodi@biochem.mpg.de (A. Aszódi).

0945-053X/03/$30.00 © 2004 Published by Elsevier B.V. on behalf of International Society of Matrix Biology.
doi:10.1016/j.matbio.2004.05.003

acterization of matrilin CC domains have revealed the potential for heterotrimeric interactions between matrilin-2 and matrilin-1 or matrilin-4 (Frank et al., 2002). The expression of matrilin-2 was demonstrated by Northern blot hybridization in various mouse organs including brain, heart, skeletal muscle, skin, and uterus, as well as in fibroblastic cell lines (Deák et al., 1997). Immunohistochemistry and in situ hybridization revealed that matrilin-2 is present in all types of loose and dense connective tissues (Piecha et al., 1999). In the skeletal system, matrilin-2 was found in the growth plate and in articular cartilages, perichondrium, periosteum, intervertebral discs, calvaria, and in osteoblasts lining the trabecular bone surface (Piecha et al., 1999; Klatt et al., 2002). In human skin, expression of matrilin-2 mRNA was found in the epidermis and dermis, while the protein was detected at the basement membrane of the epidermal–dermal junction (Piecha et al., 2002a).

The mouse and human genes coding for matrilin-2 have been recently characterized and mapped to mouse chromosome 15 (*Matn2*) and human chromosome 8q22-24 (*MATN2*), respectively (Muratoglu et al., 2000; Mátés et al., 2002). *MATN2* and *Matn2* span over 100 kb, consist of 19 exons, and both genes are transcribed from alternative promoters (Mátés et al., 2002).

The specific function of matrilins is currently unclear. In addition to the heterooligomeric interactions between the family members, matrilins have been shown to interact with both collagenous and non-collagenous matrix proteins (Winterbottom et al., 1992; Hauser et al., 1996; Piecha et al., 2002b; Wiberg et al., 2003) suggesting that matrilins could serve as general adaptor proteins in the ECM and be important for matrix assembly. Very recently, missense mutations in the exons encoding the vWFA or EGF-like domains of the human matrilin-3 gene has been identified in patients with multiple epiphyseal dysplasia (MED) (Chapman et al., 2001; Mostert et al., 2003) and hand osteoarthritis (OA) (Stefansson et al., 2003), respectively. However, matrilin-3 null mice lack skeletal abnormalities (Ko et al., 2004). Similarly, matrilin-1-deficient mice do not show an overt phenotype (Aszódi et al., 1999; Huang et al., 1999), although mild ultrastructural abnormalities of the type II collagen fibrillar network have been reported (Huang et al., 1999).

Here we report the generation and analysis of the matrilin-2-deficient mice. *Matn2* null mice are viable, have normal life spans and show no obvious abnormalities.

2. Results

2.1. Generation of matrilin-2-deficient mice

The mouse matrilin-2 gene (*Matn2*) was inactivated by homologous recombination in ES cells with a targeting vector carrying an internal ribosomal entry site-LacZ-neomycin cassette (Fig. 1a). Insertion of the targeting construct into the *Matn2* locus was designed to result in the deletion of the exon 2B containing the translation start site, the signal peptide and a positively charged region of the protein. Such a deletion was predicted to abolish the synthesis of both matrilin-2 mRNA and protein. Out of 360 ES cell clones surviving G418 selection, 18 correctly targeted ES cell clones were identified by Southern blot analysis of *Bgl*II-digested genomic DNA (Fig. 1c) using an external probe to detect a 12-kb mutant fragment and a 9-kb wild-type fragment of 129/Sv origin. Interestingly, our probe hybridized to a 6-kb wild-type band on C57BL/6 background indicating restriction enzyme polymorphism between the 129/Sv and C57BL/6 mouse strains (Fig. 1b). Chimeric males were generated using the standard techniques and subsequently crossed with C57BL/6 and 129/Sv females to produce outbred and inbred strains, respectively. Southern blot analysis of 358 offspring from heterozygous intercrosses showed the expected Mendelian ratio of genotypes (Fig. 1d). Northern blot analysis of total RNA from primary fibroblasts isolated at embryonic day E14.5 (E14.5) revealed a complete lack of *Matn2* mRNA in homozygous mutant samples (Fig. 1e).

2.2. Apparently normal embryonic development in the absence of matrilin-2

Immunohistochemical analysis at E16.5 revealed that all matrilins were expressed in the developing skeletal system in wild-type embryos (Fig. 2a). In mutant embryos, no matrilin-2 protein could be detected (Fig. 2b). Analysis of control sections treated with collagenase or protease XXIV before immunostaining showed the overlapping distribution of matrilin-2 and matrilin-4 in various non-skeletal dense and loose connective tissues including those of tendons and ligaments (Fig. 2c,c'), dermis of the skin (Fig. 2d,d'), submucosa of the intestine (Fig. 2e,e'), valves of the heart (Fig. 2f,f'), basement membranes around the main bronchus and terminal bronchioli of the lung (Fig. 2g,g'), and in the perineurium of the spinal nerves (Fig. 2h,h'). Hematoxylin-eosin (HE) staining of serial sagittal or cross sections at E14.5 and E16.5 showed an apparently normal tissue architecture in both outbred and inbred mutant embryos, which was indistinguishable from control littermates (data not shown), indicating that the absence of matrilin-2 plays do not interfere with normal embryonic development.

2.3. Endochondral bone formation and intervertebral disc development in Matn2 null mice

Adult Matn2-deficient mice showed no obvious abnormalities, were fertile, and had a normal lifespan. Since matrilin-2 is expressed during endochondral bone

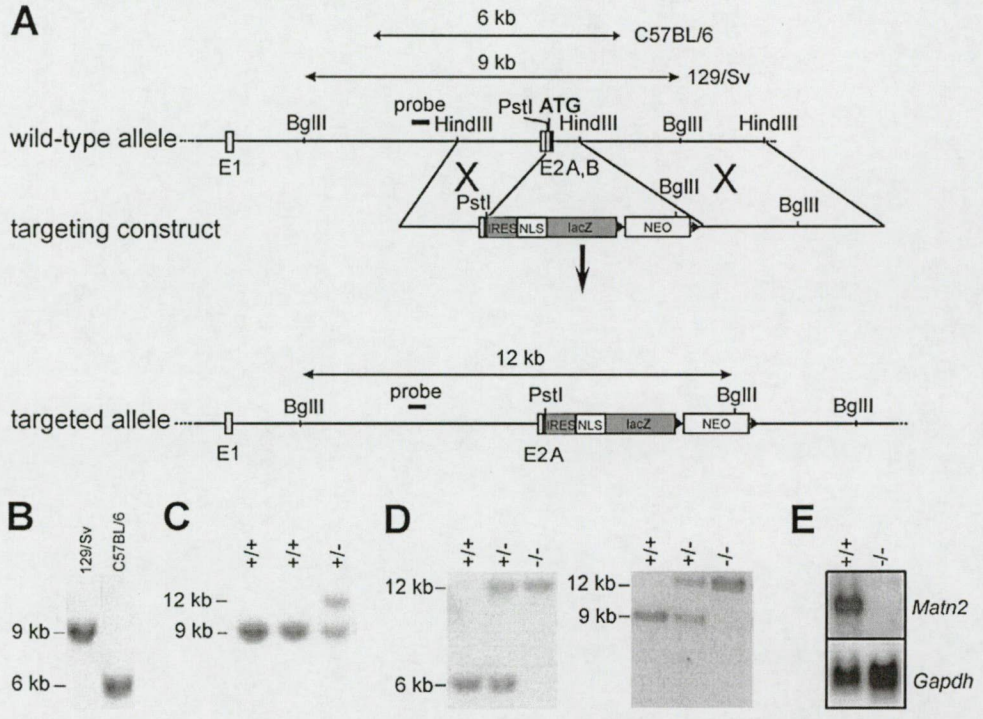

Fig. 1. Targeted inactivation of the mouse gene encoding matrilin-2. (a) Partial map of wild-type *Matn2* allele, structure of targeting vector and recombinant locus. E1 and E2 A, B indicate exons. The expected fragment sizes after *Bgl*II digestion and hybridization with an external probe are 9 kb or 6 kb for wild-type allele, depending on the genetic background, and 12 kb for recombinant allele. (b) Southern blot analysis of wild-type *Bgl*II-digested tail DNA with the external probe reveals restriction enzyme polymorphisms of the *Matn2* gene between 129/Sv and C57BL/6J mouse strains. (c) Southern blot analysis of genomic DNA from ES cell clones shows the wild-type (9 kb) and the targeted (12 kb) alleles. (d) Southern blot analysis of mouse tail DNA derived from progeny of heterozygous mating of outbred (left panel) or inbred (right panel) mice. (e) Northern blot analysis of total RNA isolated from mouse embryonic fibroblasts of wild-type (+/+) and homozygous mutant (−/−) E14.5 embryos. The blot was sequentially hybridized with probes specific for mouse *Matn2* and *Gapdh*.

formation (Fig. 2a; and in Segat et al., 2000; Klatt et al., 2002), we analyzed the development of axial and appendicular skeleton in more detail at various stages. Whole-skeleton staining with alcian blue (for cartilaginous tissues) and alizarin red (for bony tissues) at newborn stage showed no significant size alteration or skeletal malformation in the mutant compared with the control (Fig. 3a). X-ray analysis of 9-month-old mice revealed normal bone density and no abnormalities of ribs, vertebral bodies, or long bones in mutant mice (Fig. 3b). Using immunohistochemistry at E16.5, matrilin-2 was detected in the perichondrium/periosteum, at the joint surface, and weekly in the proliferative and upper hypertrophic zones of the wild type growth plate (Fig. 3c). In contrast, matrilin-1, -3 and -4 were strongly deposited throughout the cartilage. In addition, matrilin-4 expression was observed in the perichondrium/periosteum (Fig. 3c). The deposition of matrilin-1, -3, -4 (Fig. 3c) and other cartilage-specific proteins, including collagen type II and aggrecan (not shown), were apparently unchanged in the matrilin-2-deficient cartilage. Northern blot analysis of newborn limb cartilage samples revealed no obvious upregulation of *Matn2*, *-3* or *-4* gene expression (data not shown). Histological analysis of the epiphyseal and growth plate cartilages during long bone development at E16.5, newborn and various adult stages showed no detectable differences between control and homozygous mutant mice (Fig. 3d data not shown). Finally, safranin orange staining of the cartilage matrix for proteoglycans at 8 months of age showed no sign of degenerative changes at the articular surfaces (Fig. 3e).

Matrilin-2 displays strong expression during embryonic intervertebral disc (IVD) development (Piecha et al., 1999 and Fig. 2a) and in the annulus fibrosus and nucleus pulposus of adult IVDs (Deák et al., 1999). Therefore, we examined IVD development on histological sections at various embryonic and adult stages. No apparent differences between wild type and mutant IVD development were observed (Fig. 3f and data not shown).

2.4. Development of non-skeletal tissues in Matn2-deficient mice

Our previous studies revealed that matrilin-2 is expressed in various adult non-skeletal mouse tissues mainly associated with basement membrane-like struc-

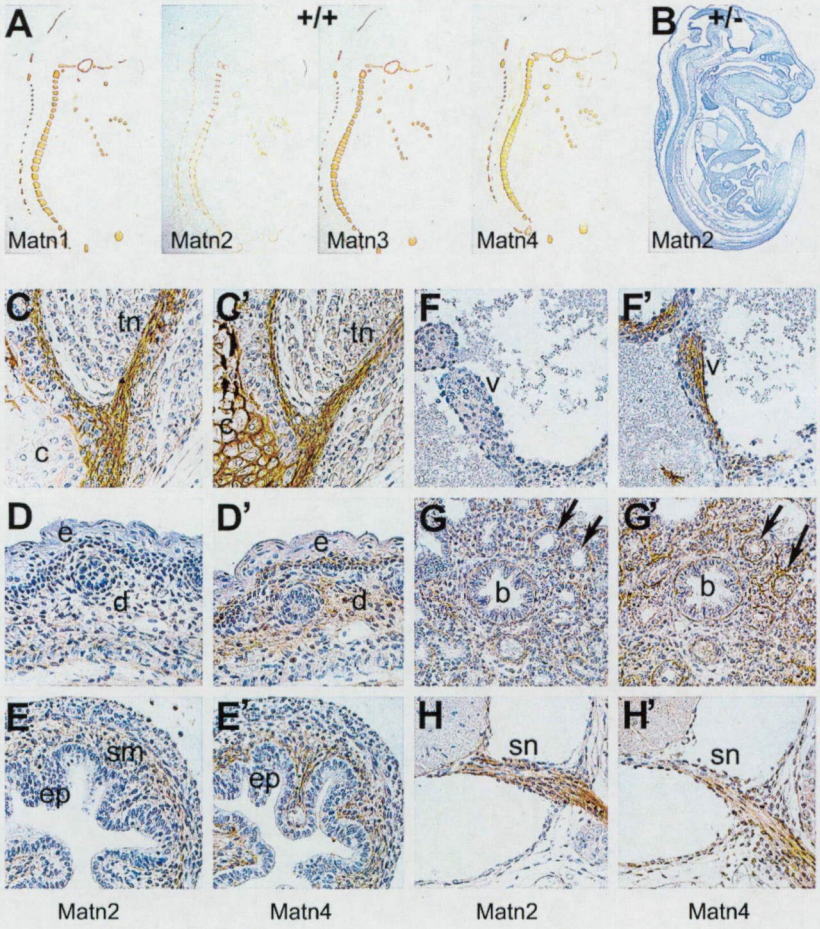

Fig. 2. Immunostaining of E16.5 mouse embryo. (a) All matrilins are expressed in the developing skeleton of a wild-type embryo. (b) Immunostaining shows the complete lack of matrilin-2 protein in a homozygous mutant embryo. The section was counterstained with hematoxylin. (c–h and c′–h′) Comparative immunostaining for matrilin-2 and matrilin-4 on collagenase-treated tissue sections of a E16.5 wild-type mouse embryo. Matrilin-2 and -4 are co-localized in tendons (tn) (c and c′), dermis (d) and epidermal–dermal junction of the skin (d and d′), submucosa (sm) of the intestine (e and e′), valves (v) of the heart (f and f′), basement membranes around the main bronchus (b) and terminal bronchioli (arrows) of the lung (g and g′), and spinal nerves (sn) (h and h′). Abbreviations: c, cartilage; e, epidermis; ep, epithelium.

tures (Deák et al., 1997; Piecha et al., 1999). In this study, the wide-ranging expression of the *Matn2* gene was further confirmed by Northern blot hybridization indicating the presence of the matrilin-2 transcripts in all investigated organs (Fig. 4a). A careful histological analysis of different non-skeletal tissues such as brain, skin, kidney, heart, lung, intestine, uterus, spleen and eye, however, showed no obvious abnormalities in mutants compared with wild-type mice (data not shown). Similarly, electron microscopic analysis of selected organs including kidney and lung revealed no ultrastructural abnormalities in Matn2-deficient mice (data not shown).

Since matrilin-4 shows a very similar expression pattern to that of matrilin-2 in adult tissues, we investigated the possible upregulation of Matn4 in Matn2 null mice. Northern and Western blot analyses of selected tissues (brain, eye and lung) at 2 months of age demonstrated that the expression levels of matrilin-4 mRNA and protein in mutant mice were comparable to those of control mice (Fig. 4b,c). To quantify more precisely the Matn4 mRNA level we employed semi-quantitative RT-PCR (Fig. 4d,e). No statistically significant differences between wild-type and mutant mice were observed for Matn4 expression in any tissues isolated from 2 weeks old animals.

2.5. The immunohistochemical distribution of the binding partners of matrilin-2 is apparently normal in the mutant skin

It has previously been shown that recombinantly expressed matrilin-2 binds various collagenous (collagens I and IV) and non-collagenous (fibronectin, laminin-1-nidogen-1 complex, fibrillin-2) components of the ECM (Piecha et al., 2002b) and that matrilin-2, at least

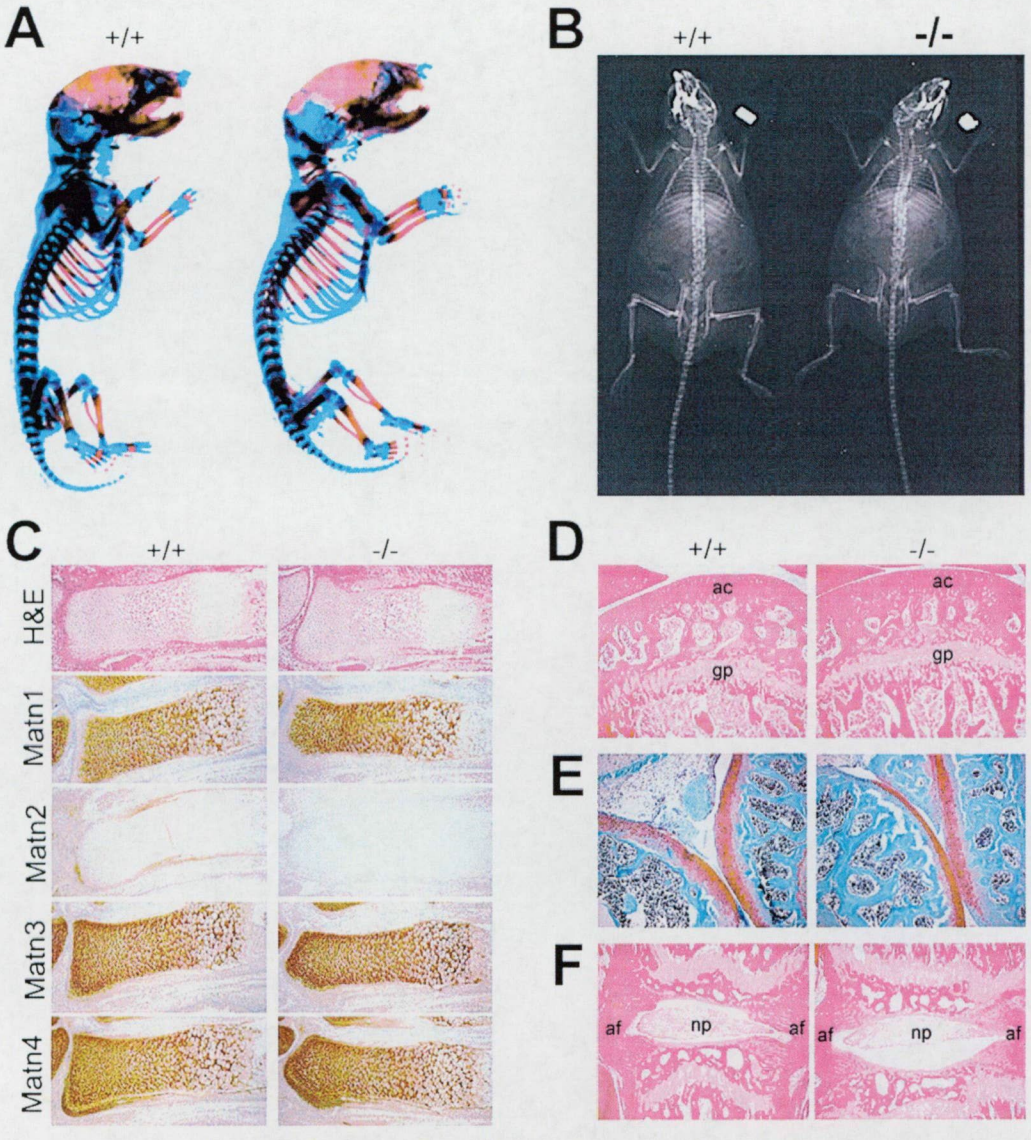

Fig. 3. Analysis of skeletal development in wild-type (+/+) and matrilin-2-deficient (−/−) mice. (a) No gross abnormalities are detectable by skeletal staining of newborn mice or by X-ray examination (b) of 9-month-old mice. (c) Hematoxilin-eosin (H&E) staining of E16.5 tibias indicates no altered cartilage morphology. Immunostaining shows matrilin-2 (Matn2) expression in the perichondrium/periosteum, at the joint surface and in the cartilage of wild-type, but not mutant tissues. The deposition of matrilin-1 (Matn1), matrilin-3 (Matn3) and matrilin-4 (Matn4) is comparable in wild-type and mutant cartilage. (d) H&E staining and Safranin orange staining (e) indicate no degeneration or altered proteoglycan content of the articular cartilage (ac) at 8-months of age; gp, growth plate. (f). H&E staining shows normal intervertebral disc formation in 4-month-old mutant. Abbreviations: af, annulus fibrosus; np, nucleus pulposus.

partially, co-localizes with collagens I and IV, fibronectin, and fibrillin-1 in the skin in vivo (Piecha et al., 2002a). These observations prompted us to compare the distribution of these putative matrilin-2 binding ligands in wild-type and mutant adult skin. In wild-type mice, matrilin-2 was strongly deposited at the epidermal–dermal junction, around hair follicles, vessels, and sebaceous glands, whereas a very weak expression was observed in the upper part of the dermis (Fig. 5a). Matrilin-4 displayed similar tissue distribution with additional strong expression in the whole epidermis and the upper dermis (Fig. 5c). Mutant skin lacked matrilin-2 expression (Fig. 5b) and showed normal matrilin-4 immunostaining (Fig. 5d). The expression of the potential ligands for matrilin-2, like the basement membrane components laminin-1 (Fig. 5k,l), nidogen-1 (Fig. 5m,n), collagen IV (Fig. 5o,p), the microfibrillar constituent fibrillin-2 (Fig. 5i,j), and the major dermal ECM proteins collagen I and fibronectin, was also indistinguishable between wild-type and mutant animals. Fur-

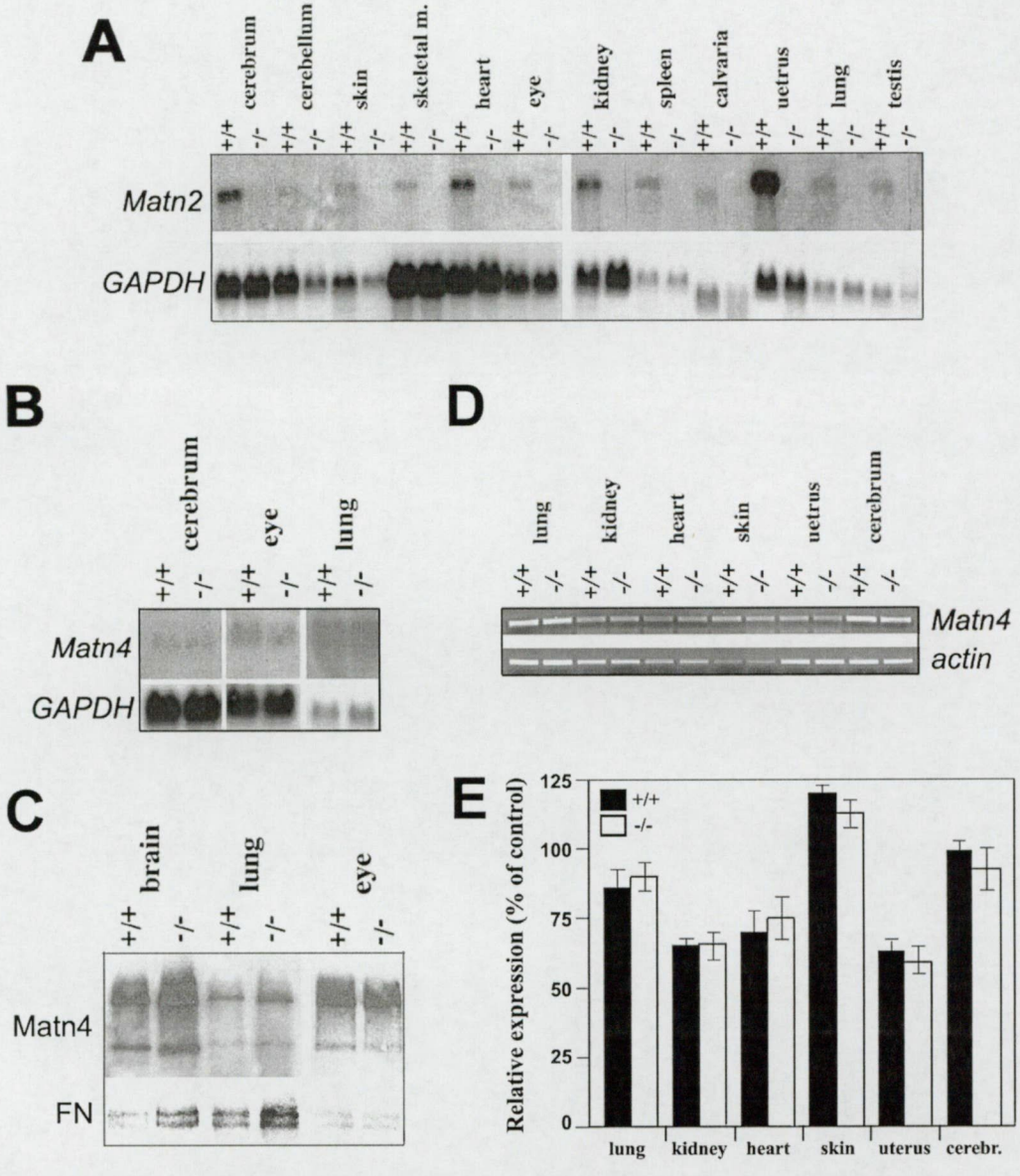

Fig. 4. Expression analyses. (a) Northern blot analysis at 2-months of age demonstrate the expression of matrilin-2 mRNA in all investigated organs of wild-type (+/+) mice, whereas no *Matn2* transcript was detectable in mutant (−/−) samples. (b) Northern and (c) Western blot analyses show no upregulation of matrilin-4 mRNA or protein levels in *Matn2* null extracts. (d) Representative RT-PCR analysis of *Matn4* expression in +/+ and −/− tissues. (e) Quantification of the Matn4 major transcript as relative mRNA level normalized to beta-actin gene expression. Data are expressed as the mean ±S.D.

thermore, ultrastructural analysis indicated intact basement membrane at the epidermal–dermal junction (Fig. 6b) and normal organization of dermal collagen fibrils in mutant skin (Fig. 6d).

3. Discussion

The members of the matrilin family of ECM proteins can form both collagen-dependent and collagen-independent fibrillar networks (Winterbottom et al., 1992; Chen et al., 1995; Piecha et al., 1999; Klatt et al., 2000, 2001) and are involved in a variety of protein–protein interactions (Winterbottom et al., 1992; Hauser et al., 1996; Piecha et al., 2002b; Wiberg et al., 2003). Matrilin-2, a ubiquitously expressed family member, interacts with various collagenous (collagens I and IV) and non-collagenous proteins (fibrillin-2, fibronectin, and laminin-1-nidogen-1 complexes) in vitro (Piecha et al., 2002b) suggesting that matrilin-2 may perform an important function as adaptor protein in the supramolec-

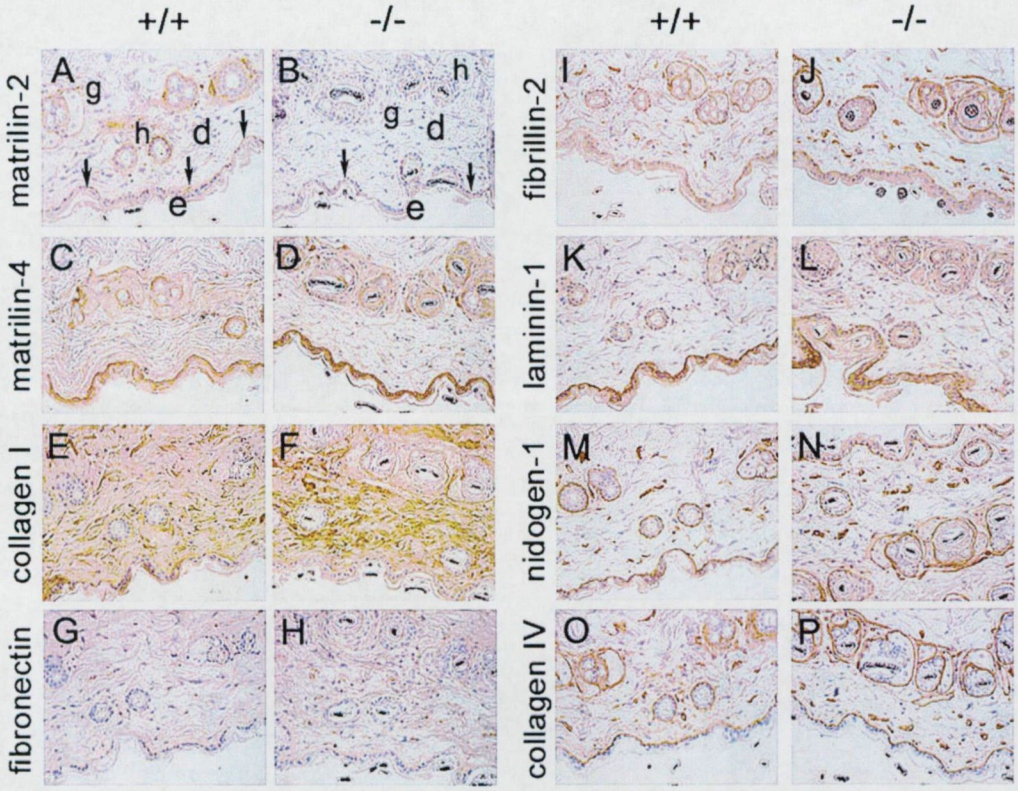

Fig. 5. Deposition of matrilin-2 ligands is apparently normal in mutant skin. Sections of wild-type (+/+) and mutant (−/−) adult skin were immunostained with antibodies against matrilin-2 and its various binding partners. The sections were counterstained with hematoxylin. Abbreviations: d, dermis; e, epidermis, h, hair follicle; g, gland; arrows indicate the epidermal–dermal junction.

ular organization of the ECM. To assess the in vivo relevance of such an adaptor function of matrilin-2, we generated matrilin-2-deficient mice.

Matn2 null mice are viable, fertile, and display an apparently normal phenotype. Careful histological analyses at various embryonic and postnatal stages did not reveal any obvious alterations in architecture of mutant tissues. Furthermore, we have not found ultrastructural abnormalities in mutant tissues such as lung, kidney and skin. These results indicate that matrilin-2 is not essential for development and proper tissue function.

In this study, we show that matrilin-2 is abundant in the dermis and at the epidermal–dermal junction of embryonic skin, while in adult tissues, its deposition is mostly restricted to the basement membrane underlying the epidermis and around the skin appendages. This observation suggests that the localization of the matrilin-2 protein is developmentally regulated in the skin. During embryogenesis, matrilin-2 might play a role in the establishment and the correct assembly of the dermis and epidermal–dermal junctions, while in adult skin, its function is likely more related to the stabilization of the basement membranes. Such a role of matrilin-2 in the skin is supported by the interaction and the partial co-localization of matrilin-2 with collagen I and fibronectin (the major ECM components of the dermis), basement membrane constituents such as laminin-1-nidogen-1 complexes and collagen type IV, and with the microfibrillar components fibrillin-1 and -2 (Piecha et al., 2002a). However, since we observed normal skin ultrastructure and deposition of matrilin-2 ligands in the Matn2 null mice, we conclude that the hypothetic role of matrilin-2 is either not important for skin development or its function is shared by other matrix molecules.

The lack of an apparent phenotype in the Matn2 null mice could be explained by the overlapping expression and, therefore, redundant function of matrilins. In skeletal tissues, matrilin-2 is weakly deposited in the proliferative and upper hypertrophic zones of the cartilaginous growth plate where all other matrilins (matrilin-1, -3 and -4) are also present (Klatt et al., 2002). Matrilin-2 displays strong expression and co-localization with matrilin-4 in the perichondrium, periosteum and at the articular surface of the joints (Klatt et al., 2002 and Fig. 3c). Outside of the skeleton, matrilin-4 is expressed and partially colocalized with matrilin-2 in most tissues during embryonic and adult development. Compensatory upregulation of structurally related molecules in mice

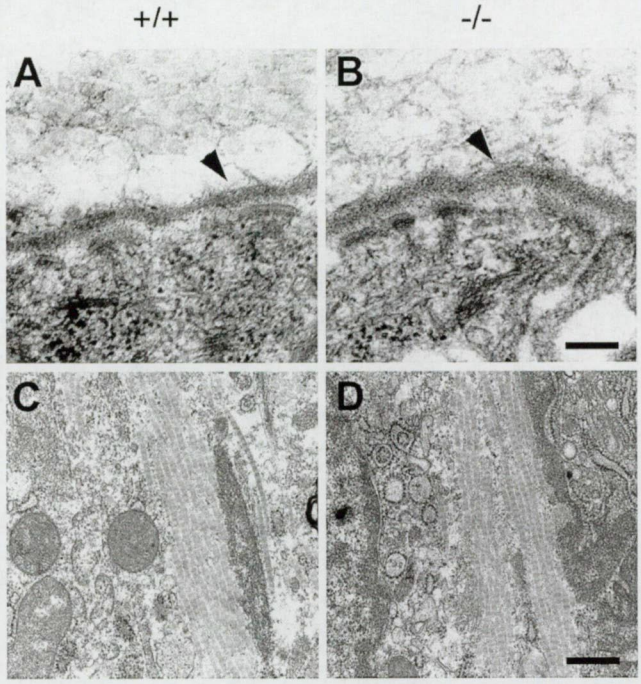

Fig. 6. Ultrastructural analysis of adult skin. Transmission electron micrographs of back skin of wild type (a, c) and mutant (b, d) mice indicate that the appearance of epidermal–dermal junction (arrow, b) and the morphology and density of dermal collagen fibrils (d) are normal in Matn2 null mice.

null for a variety of ECM proteins has been widely reported. For example, in fibromodulin-null mice, a four-fold increase of lumican protein level was observed in tail tendons (Svensson et al., 1999). In nidogen 1 knockout mice, the level of nidogen 2 increased in certain basement membranes (Murshed et al., 2000). However, we found no sign of significant upregulation of Matn1, Matn3 and Matn4 mRNA or protein levels in Matn2 null tissues implying that matrilin-2-deficiency might be compensated by the steady-state levels of other members of the matrilin family. This hypothesis is further supported by the observation that matrilins can form heterooligomers and by the lack of overt phenotype and compensatory upregulation in the Matn1 and Matn3 null mice (Aszódi et al., 1999; Ko et al., 2004). To resolve the question of redundancy among the matrilins, the generation of compound matrilin knockout mice is in progress in our laboratory.

The apparently normal development and tissue architecture of the *Matn2* null mice do not exclude the possibility that matrilin-2 plays a more obvious role in mice under challenging conditions. To assess the function of matrilin-2 in skin wounding, bone fracture healing, or in tissues under excess mechanical loading, further studies are required. Alternatively, the genetic background could also affect the manifestation of the phenotype. Although we observed no differences between outbred (C57BL6/129Sv) and inbred (129Sv) matrilin-2-deficient mouse strains, the impact of the mutation on a pure C57BL6 background is remains to be elucidated.

4. Experimental procedures

4.1. Generation of matrilin-2-deficient mice

Genomic clones of *Matn2* encoding matrilin-2 were isolated from 129/Sv libraries as described (Mátés et al., 2002). The gene was disrupted by inserting a cassette with a ribosomal re-entry site (IRES), a lacZ reporter gene with a nuclear localization signal (NLS), and a floxed neomycin (NEO) cassette into the PstI-HindIII sites, thereby deleting the ATG motif and the nucleotide sequences coding for the signal peptide of exon 2B (Fig. 1a). R1 embryonic stem (ES) cells derived from a 129/Sv mouse strain were electroporated with the linearized targeting vector DNA and selected with 500 μg/ml G-418 in ES cell culture media. Genomic DNA isolated from the ES cell clones surviving the selection were digested with *Bgl*II and analysed by Southern blot hybridization using an 800-bp external probe (Fig. 1a). The probe was designed to detect a 12-kb mutant band and a 9-kb wild type band. Two correctly targeted clones were microinjected into blastocysts to generate male chimeras, which were subsequently mated with C57BL/

6 and 129/Sv females to establish outbred and inbred *Matn2*-null mice, respectively.

4.2. RNA analysis

Total RNA was isolated from various adult organs and embryonic primary fibroblasts as described previously (Aszódi et al., 1996). For Northern analysis, 5–20 μg of total RNA was size fractionated on a 1% agarose-2.2 M formaldehyde gel and transferred to Hybond N+ membrane (Amersham). Filters were hybridized with P^{32}-labeled cDNA probes specific for matrilin-1, -2, -3 (Aszódi et al., 1999), matrilin-4 (Wagener et al., 1997) and glyceraldehyde phosphodehydrogenase. For semiquantitative RT-PCR, two micrograms of total RNA were transcribed into cDNA using the SuperScript™ III RNaseH$^-$ reverse transcriptase (Invitrogen). For PCR reactions, 0.5 unit AmpliTaq DNA polymerase (Invitrogen) and 2 μl cDNA were used in 50 μl amplification buffer containing 0.2 mM dNTPs, 1.5 mM $MgCl_2$ and 200 μM each of forward and reverse primers. The primer pairs specific for exon 0b of the mouse *Matn4* gene were described previously (Wagener et al., 2001). The primer pairs specific for beta-actin were: 5′-TGACGGGGTCACCCACAC-3′ (forward) and 5′-CTAGAAGCATTTGCGGTG-GAA-3′ (reverse). PCR was performed using the PTC-200 Peltier Thermal Cycler (MJ Research) under the following conditions: 94 °C for 4 min, 94 °C for 1 min, 60 °C for 1 min and 72 °C for 1 min, 35 cycles for *Matn4* and 20 cycles for beta-actin, followed by 72 °C for 10 min. PCR reactions were repeated three times and relative mRNA levels were determined by optical densitometry using the Bio-Profile computer-assisted imaging system (Vilber Lourmat).

4.3. Histology and immunohistochemistry of embryonic and adult non-skeletal tissues

The histological and immunohistochemical analyses were conducted on both C57BL6/129Sv and 129/Sv genetic backgrounds. For histology, 14.5-, 15.5-, and 16.5-day-old embryos and various organs form 1-, 2-, and 4-month-old mice were fixed in 4% paraformaldehyde (PFA) in phosphate-buffered saline (PBS, pH 7.2). After paraffin embedding, sections of 6 μm were cut and stained with hematoxylin-eosin (H&E). For each stages, at least three wild-type and mutant samples were analyzed using serial sections representing the embryonic or adult tissues.

For immunohistochemistry, samples were fixed in 95% ethanol-5% glacial acetic acid and embedded in paraffin. Immunostaining was performed by the avidin-biotin complex (ABC) procedure using a commercially available kit (Vectastain). To improve antibody penetration to the tissue, sections were routinely digested before immunostaining with protease XXIV (10 μg/ml in PBS, Sigma) for 20 min or with collagenase (5 μg/ml, collagenase type II, Worthington) for 5 min at 37 °C. Rabbit polyclonal antibodies against the following antigens were used: matrilin-1, matrilin-2, matrilin-3, matrilin-4 (see Ko et al., 2003, and references therein); collagen I, collagen IV, laminin-1, nidogen-1 (all kindly provided by Dr Rupert Timpl, MPI, Martinsried, Germany) and fibrillin-2 (kind gift from Dr Dieter P. Reinhard, University of Lübeck, Lübeck, Germany).

4.4. Skeletal analysis

Skeletal staining of newborn mice with alcian blue/alizarin red and X-ray analysis of adult mice were performed as previously described (Aszódi et al., 1999). For histology, adult bones were fixed in 4% PFA, decalcified in 10% EDTA and stained with H&E or Safranin Orange-Weigert hematoxylin. Immunostaining of skeletal tissues with antibodies against matrilin-1, -2, -3 and -4, collagen type II and aggrecan was performed as previously described (Aszódi et al., 1999).

4.5. Ultrastructural analysis

For electron microscopy, tissue samples were fixed in 0.15 M sodium cacodylate buffer, pH 7.4, containing 2.5% glutaraldehyde for 1 day at room temperature. They were subsequently rinsed three times in isotonic sodium cacodylate buffer for 30 min and postfixed in 0.15 M sodium cacodylate, pH 7.4, containing 1% (wt/vol) osmium tetroxide for 2 h. Samples were then rinsed in isotonic buffer solution, dehydrated in a graded series of ethanol, and embedded in Epon 812. Semithin (1 μm) and thin (60 nm) sections were cut on a Leica Ultracut S (Deerfield, IL). Sections were stained in 5% uranyl acetate for 2 h and then in a saturated lead citrate solution for 7 min. All samples were viewed in a Jeol1200 EX transmission electron microscope operated at 60-kV accelerating voltage.

4.6. Biochemical analysis

Various organs from 1- and 3-month-old mice were homogenised in buffer containing 0.25 M NaCl, 50 mM Tris–HCl (pH 7.4) and 10 mM EDTA and extracted with gentle agitation for 1.5 h at 37 °C after the addition of 2 mg/ml collagenase type II. Unextracted material was removed by centrifugation at 8000×*g* for 10 min at 4 °C. Nonreducing SDS-polyacrylamide gel electrophoresis sample buffer (5x) was added to the samples and the proteins were separated on 7% SDS-polyacrylamide gels then blotted onto Trans-Blot nitrocellulose membranes (Bio-Rad). The blots were subsequently hybridized with polyclonal antibodies specific for matrilin-2, -4 and tubulin or fibronectin as a control for

protein loading. Bound antibodies were hybridized to horseradish peroxidase-conjugated swine anti-rabbit immunoglobulin G (Sigma) and detected using the enhanced chemiluminescence (ECL) kit (Amersham).

5. Uncited reference

Wagener et al., 1998

Acknowledgments

We thank C. Cramnert, K. Sakai, A. Simon, I. Kravjár, I. Fekete and Zs. Farkas for technical assistance, Dr Éva Kemény, Dr. Kathryn Rodgers for reading the manuscript, and Dr Reinhard Fässler (MPI, Dept. of Molecular Medicine) for supporting the project. This study was supported by grants from OTKA T022224, T029142, T034399 and T034729 from the Hungarian National Scientific Research Foundation to I.K. and F.D.; by the National Research and Development Program NKFP-1A/0023/2002 to I. K.; by the Max-Planck Society, the Deutsche Forschungsgemeinschaft (AS 150/1-1; 436 UNG 113/154/2-1), the Swedish Medical Research Council, the Anna-Greta Crafoords Foundation, the Greta and Johan Kocks Foundation to A.A.; and by a short term fellowship from EMBO to L.M.

References

Aszódi, A., Hauser, N., Studer, D., Paulsson, M., Hiripi, L., Bösze, Z., 1996. Cloning, sequencing and expression analysis of mouse cartilage matrix protein cDNA. Eur. J. Biochem. 236, 970–977.

Aszódi, A., Bateman, J.F., Hirsch, E., Baranyi, M., Hunziker, E.B., Hauser, N., et al., 1999. Normal skeletal development of mice lacking matrilin 1: redundant function of matrilins in cartilage? Mol. Cell Biol. 19, 7841–7845.

Chapman, K.L., Mortier, G.R., Chapman, K., Loughlin, J., Grant, M.E., Briggs, M.D., 2001. Mutations in the region encoding the von Willebrand factor A domain of matrilin-3 are associated with multiple epiphyseal dysplasia. Nat. Genet. 28, 393–396.

Chen, Q., Johnson, D.M., Haudenschild, D.R., Tondravi, M.M., Goetinck, P.F., 1995. Cartilage matrix protein forms a type II collagen-independent filamentous network: analysis in primary cell cultures with a retrovirus expression system. Mol. Biol. Cell 6, 1743–1753.

Deák, F., Piecha, D., Bachrati, C., Paulsson, M., Kiss, I., 1997. Primary structure and expression of matrilin-2, the closest relative of cartilage matrix protein within the von Willebrand factor type A module superfamily. J. Biol. Chem. 272, 9268–9274.

Deák, F., Wagener, R., Kiss, I., Paulsson, M., 1999. The matrilins: a novel family of oligomeric extracellular matrix proteins. Matrix Biol. 18, 55–66.

Frank, S., Schulthess, T., Landwehr, R., Lustig, A., Mini, T., Jenö, P., et al., 2002. Characterization of the matrilin coiled-coil domains receals seven novel isoforms. J. Biol. Chem. 277, 19071–19079.

Hauser, N., Paulsson, M., Heinegård, D., Mörgelin, M., 1996. Interaction of cartilage matrix protein with aggrecan: increased covalent cross-linking with tissue maturation. J. Biol. Chem. 271, 32247–32252.

Huang, X., Birk, D.E., Goetinck, P.F., 1999. Mice lacking matrilin-1 (cartilage matrix protein) have alterations in type II collagen fibrillogenesis and fibril organization. Dev. Dynam. 216, 434–441.

Klatt, A.R., Nitsche, P.D., Kobbe, B., Mörgelin, M., Paulsson, M., Wagener, R., 2000. Molecular structure and tissue distribution of matrilin-3, a filament-forming extracellular matrix protein expressed during skeletal development. J. Biol. Chem. 275, 3999–4006.

Klatt, A.R., Nitsche, D.P., Kobbe, B., Macht, M., Paulsson, M., Wagener, R., 2001. Molecular structure, processing and tissue distribution of matrilin-4. J. Biol. Chem. 276, 17267–17275.

Klatt, A.R., Paulsson, M., Wagener, R., 2002. Expression of matrilins during maturation of mouse skeletal tissues. Matrix Biol. 21, 289–296.

Ko, Y., Kobbe, B., Nicolae, C., Miosge, N., Paulsson, M., Wagener, R., et al., 2004. Matrilin-3 is dispensable for mouse skeletal growth and development. Mol. Cell Biol. 24, 1691–1699.

Mátés, L., Korpos, É., Deák, F., Liu, Z., Beier, D.R., Aszódi, A., et al., 2002. Comparative analysis of the mouse and human genes (*Matn2* and *MATN2*) for Matrilin-2, a filament-forming protein widely distributed in extracellular matrices. Matrix Biol. 21, 163–174.

Mostert, A.K., Dijkstra, P.F., Jansen, B.R.H., van Horn, J.R., de Graaf, B., Heutink, P., et al., 2003. Familial multiple epiphyseal dysplasia due to a matrilin-3 mutation: Further delineation of the phenotype including 40 years follow-up. Am. J. Med. Genet. 120A, 490–497.

Muratoglu, S., Krysan, K., Balázs, M., Sheng, H., Zákány, R., Módis, L., et al., 2000. Primary structure of human matrilin-2, chromosome location of the *MATN2* gene and conservation of an AT-AC intron in matrilin genes. Cytogenet. Cell Genet. 90, 323–327.

Murshed, M., Smyth, N., Miosge, N., Karolat, J., Krieg, T., Paulsson, M., et al., 2000. The absence of nidogen 1 does not affect murine basement membrane formation. Mol. Cell Biol. 20, 7007–7012.

Piecha, D., Muratoglu, S., Mörgelin, M., Hauser, N., Studer, D., Kiss, I., et al., 1999. Matrilin-2, a large, oligomeric matrix protein, is expressed by a great variety of cells and forms fibrillar networks. J. Biol. Chem. 274, 13353–13361.

Piecha, D., Hartmannm, K., Kobbe, B., Haase, I., Mauch, C., Krieg, T., et al., 2002a. Expression of matrilin-2 in human skin. J. Invest. Dermatol. 119, 38–43.

Piecha, D., Wiberg, C., Mörgelin, M., Reinhardt, D.P., Deák, F., Maurer, P., et al., 2002b. Matrilin-2 interacts with itself and with other extracellular matrix proteins. Biochem. J. 367, 715–721.

Segat, D., Nitsche, P.D., Klatt, A.R., Piecha, D., Korpos, E., Deák, F., et al., 2000. Expression of matrilin-1, -2 and -3 in developing mouse limbs and heart. Matrix Biol. 19, 649–655.

Stefansson, S.E., Jonsson, H., Ingvarsson, T., Manolescu, I., Jonsson, H.H., Olafsdottir, G., et al., 2003. Genomewide scan for hand osteoarthritis: a novel mutation in matrilin-3. Am. J. Hum. Genet. 72, 1448–1459.

Svensson, L., Aszódi, A., Reinholt, F.P., Fässler, R., Heinegård, D., Oldberg, A., 1999. Fibromodulin-null mice have abnormal collagen fibrils, tissue organization, and altered lumican deposition in tendon. J. Biol. Chem. 274, 9636–9647.

Wagener, R., Kobbe, B., Paulsson, M., 1998. Matrilin-4, a new member of the matrilin family of extracellular matrix proteins. FEBS Lett. 436, 123–127.

Wiberg, C., Klatt, A.R., Wagener, R., Paulsson, M., Bateman, J.F., Heinegård, D., et al., 2003. Complexes of matrilin-1 and biglycan or decorin connect collagen VI microfibrils to both collagen II and aggrecan. J. Biol. Chem. 278, 37698–37704.

Winterbottom, N., Tondravi, M.M., Harrington, T.L., Klier, F.G., Vertel, B.M., Goetinck, P.F., 1992. Cartilage matrix protein is a component of the collagen fibril of cartilage. Dev. Dynam. 193, 266–276.